Late Weichselian glacial and geomorphological reconstruction of South-Western Scania, Sweden

Kilian Barth

**Masters thesis in Geology at Lund University,
no. 273
(45 hskp/ECTS)**

**Department of Earth- and Ecosystem Sciences
Division of Geology
Lund University**
2011

Late Weichselian glacial and geomorphological reconstruction of South-Western Scania, Sweden

Master Thesis

Kilian Barth

Division of Geology
Department of Earth and Ecosystem Sciences
Lund University

2011

Contents

Cover Picture: Calcite draping on the upper boundary of Subunit 2e

Late Weichselian glacial and geomorphological reconstruction of South-Western Scania, Sweden

KILIAN BARTH

Barth, K., 2010: Late Weichselian glacial and geomorphological reconstruction of South-Western Scania, Sweden. *Examensarbeten i geologi vid Lunds universitet*, Nr. 267??, 28 pp., 45 points.

Abstract: This study was carried out to deliver new insight into the late Weichselian landscape development of South-Western Scania and to make regional scale glaciation models of South-Western Scandinavia more accurate.

The goal of this study is to find out how the latest ice advances affected the study area. Until now, it was unclear if all ice advances overrode all parts of the study area or if different areas were affected differently.

The reconstructions presented in this paper are based on an interpretation of the geomorphology and on a sedimentological analysis of a section in Vellinge. The investigated parameters were sedimentary structures, clast provenance and deformation structures. These results were then used to reconstruct the depositional environments.

Two diamicts divided by a unit of sorted sediments were observed in Vellinge. While the diamicts are interpreted as subglacial deformation tills formed by two different ice advances from the Baltic basin, the sediments in between represent a deglaciation sequence.

All of the area was overridden by the early stages of the young-Baltic ice advances. Those earlier advances left behind dead-ice in the areas that are hummocky today. This dead-ice diverted the latest stages of the ice advances which only reached the coastal plains. These advances were ice streams and formed the present landscape in their subglacial system while the areas further inland kept their hummocky appearance.

These results imply thin and highly dynamic ice streams for the last part of the late Weichselian. They also imply an early and rapid deglaciation of central Scania.

Keywords: Late Weichselian, ice lobe, ice stream, Scania, Vellinge, Trelleborg, Malmö

Kilian Barth, Division of Geology, Department of Earth and Ecosystem Sciences, Lund University, Sölvegatan 12, SE–223 62 Lund, Sweden. E-mail: kbarth@fto.de

Rekonstruktion av glacial utveckling och geomorfologi av sydvästra Skåne under den sen Weichseltid

KILIAN BARTH

Barth, K., 2010: Late Weichselian Landscape History of South-Western Scania, Sweden. (Rekonstruktion av glacial utveckling och geomorfologi av sydvästra Skåne under den sen Weichseltid) *Examensarbeten i geologi vid Lunds universitet*, Nr. 267??, 28 pp.., 45 poäng.

Sammanfattning: Denna studie utfördes för att få nya insikter i syd-västra Skånes landskapsutveckling under slutfasen av Weichselistiden i syfte att göra existerande regionala glaciationsmodeller pålitligare. Undersökningen inriktades på att utröna hur sydvästra Skåne påverkades av senaste istidens sista isframstötar då det genom tidigare studier inte varit helt klart om dessa överskred hela undersökningsområdet eller endast påverkade delar av detsamma. De modellerna som framställs i detta arbete grundar på sedimentologiska undersökningar utförda i ett vägschakt i Vellinge samt geomorfologisk tolkning av landskapselement i närområdet.

I schaktet påvisades två diamikta enheter, tolkade som subglacialt avsatt morän vid två olika baltiska isframstötar som täckte hela undersökningsområdet från sydlig riktning. Dessa moräner mellanlagras av sorterade sediment, avsatta i samband med avsmältningen av isen från den tidigare isframstöten. I samband med den första baltiska isframstöten avskildes stagnant is i nord och nordost om området kring Vellinge, ett område som kallas 'backlandskapet' på grund av sin kulliga topografi. Denna dödis avlänkade den senare isframstöten, varför denna enbart överskred de kustnära områden av södra Skåne och formade nutidens subglacialt bildade slättlandskap, medan de områden som är belägna längre in i landet bevarade sitt toppiga utseende från utsmältning av is från den första baltiska isframstöten. Dessa resultat indikerar tunna och högdynamiska isströmmar under Weichselistidens slutfas och också en tidig och snabb isavsmältning av Skånes centrala delar.

Nyckelord: Skåne, Weichsel, Söderslätt, Backlandskapet, Vellinge, Trelleborg, Malmö, isström

Kilian Barth, Enheten för geologi, Institutionen för geo- och ekosystemvetenskaper, Lunds universitet, Sölvegatan 12, 223 62 Lund, Sverige. E-post: kbarth@fto.de

1 Introduction

South-Western Scania is an area in which geological research has been carried out over a long time. Results on the Quaternary developments have been published from both sides of Öresund, the Danish and the Swedish one. Most of the recent reconstructions are mainly based on Danish data (e.g. Houmark-Nielsen & Kjær 2003; Larsen et al. 2009).

The conceptual models of the developments during the Late Weichselian generally agree that there were two ice advances after the main advance from the north east, named the East Jylland advance and the Bælthav advance after the location of their respective ice marginal lines. The Main Stationary Line (MSL) represents the Last Glacial Maximum (LGM) in Denmark and is interpreted to represent a thick and slowly flowing part of the Scandinavian Ice Sheet (SIS). The younger ice-marginal lines are thought to be related to lobate shaped, terrestrial based terminal parts of thin and low-gradient Younger Baltic ice-streams. In the Öresund region one more ice advance is recorded in the stratigraphy (Kjær et al. 2003).

The continuation into south Sweden of the marginal lines of those younger advances, as recorded in Denmark, is still under debate, and the correlation to glacial sediments and landforms in Scania is still unclear.

Two fundamentally different reconstructions of glacier development have been suggested (Fig. 1). The first one suggests ice lobes distinctly separated from the SIS and strongly protruding (Ringberg 1989), whereas the second one suggests ice-lobes with a closer connection to the main ice sheet (Houmark-Nielsen & Kjær 2003). While the first alternative implies an early deglaciation of central Scania and a gradual melting north of it, the second alternative implies a later and slower deglaciation of central Scania due to a thicker ice in the north. As these two reconstructions are not only important for the glacial history of Scania, but also for understanding the history of the larger region of southern Sweden and the southwestern Baltic, more data are needed to evaluate the validity of these models.

The aim of this study is to collect more data in a key area of the low-lying coastal region of south-western Scania to find out how it was affected by the latest ice advances.

The geomorphology and glacial stratigraphy of the area are analysed and the sedimentology of a representative section is presented, aiming to resolve glacial dynamics and ice-flow pattern related to the Young Baltic ice-lobe.

2 Previous studies

The first investigations of the glacial history of southern Sweden were published by Holst and Holmström at the turn of the 20th century (e.g. Holmström 1896, 1899, 1904; Holst 1895, 1903, 1911a, 1911b). While Holst proposed a theory of one single glaciation and ice advance, Holmström favoured a system of several ice advances and retreats. This more complex system has also been supported by Munthe (1920) and Nilsson (1959) and in general is still accepted by many authors (e.g. Kjær et al. 2003, 2006).

Nilsson (1959) assigned the Quaternary sediments to different ice advances and retreats. This was done by interpretation of lithology and directional elements and a re-interpretation of older data. According to Nilsson (1959), the oldest sediments, including the infill of the Alnarp Valley, have a Baltic provenance. This older Baltic advance was followed by an ice advance from north and northeast. Finally, the study area was overridden by younger Baltic advances called the higher, middle and lower. The main problem with the older reconstructions and the one by Nilsson is that they lack absolute chronology and only provide a relative chronology.

Lagerlund (1977a,b) criticised that many of the older results are too much focused on striations and indicator pebbles. He found that there is a discrepancy between older, indicator based boundaries and the surface topography, and argued that studies of clast provenance by means of fine gravel analysis and an investigation of "neotectonics" are necessary to find out more details about the glacial history of Scania and especially about the lateral extent of the Baltic ice advances.

Lagerlund (1987) suggested that Scania was ice free during the early and middle Weichselian and became glaciated first after 21 ka BP. He stated that the NE origin of the main ice advance was the dominant movement direction during the whole glaciation and that the East Jylland advance, the Bælthav advance and the Simrishamn advance need to be explained by the formation and collapse of marginal ice domes on top of stagnant ice during general deglaciation. He interpreted the long transported Baltic erratics as being partly transported by the advance of the ice-domes themselves and partly by ice streams that formed between the ice domes and stagnant ice surrounding them. According to Lagerlund (1987), the Low Baltic ice stream, as suggested in earlier literature, never existed.

Malmberg Persson and Lagerlund (1990) continued this argument and proposed a glacioaquatic deposition of what formerly had been suggested to represent the last, (sub-) glacial deposition in the area (the 'Low Baltic' till). These deposits were renamed as 'Lund Diamicton'. That means that the Lund diamicton is not equivalent to a 'Low Baltic' till and would not have been deposited by a 'Low Baltic ice stream'. They concluded that the maximum distribution of the Lund diamicton does *not* represent the margin of a glacier advance, but instead the highest coastline for the glacioaquatic basin into which the Lund diamicton was deposited.

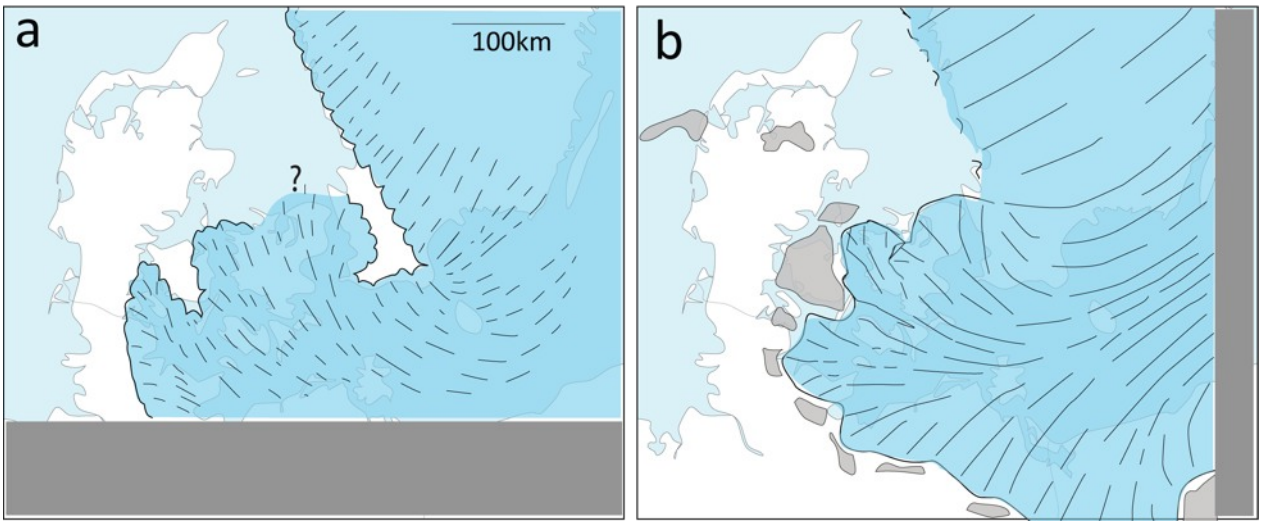

Fig. 1. Two models of ice-lobe distribution in the southern Baltic basin during the Late Weichselian. a: Distinctly separated, strongly protruding ice lobe (modified after Ringberg 1989) b: Ice lobe with a close connection to the main ice sheet, modified after Houmark-Nielsen & Kjær (2003); the grey polygons depict dead-ice. The grey rectangles are areas not covered by the respective model.

Further, more local studies exist on the Quaternary deposits in the lime stone quarry in Limhamn (Adrielsson et al. 1989) and for the sections exposed in connection with the construction of the Öresund bridge (Jönsson 2000).

For the Upper Weichselian, Houmark-Nielsen (1999) developed a lithostratigraphy consisting of 'Mid Danish till', 'East Jylland till' and 'Bælthav till'. The first one was deposited during an advance of the Scandinavian Ice Sheet (SIS), whereas the latter two were deposited during phases of general deglaciation.

Kjær et al. (2003) examined the last three advances of the SIS during the Late Weichselian and claimed that the main advance from central Sweden (with an age of *c.* 21–20 ka BP) was a 'relatively slow-flowing inter-stream ice body' which had high bed interaction, while the Baltic advances were interpreted as being rapidly flowing ice-streams which had limited bed interaction. They also found that the flow lines of the SIS became successively more fan-shaped, indicating an increasing influence of subglacial topography. The authors related this change in the flow lines to a decreased thickness of the ice.

Houmark-Nielsen & Kjær (2003) provided palaeogeographical reconstructions for a timespan of 40–15 ka BP for the region of south-western Scandinavia. They based their model on the lithostratigraphy of 'tills and inter-till sediments' and provided ages achieved by optically stimulated luminescence (OSL) and radiocarbon (^{14}C) measurements. They argued that ice streams are the main drainage ways for the SIS and placed the last ice advance in the area of easternmost Denmark and the Öresund region at an age of slightly before 16 ka BP. They stated that this advance started as a surge of a lobe of the Bælthav ice stream.

Kjær et al. (2006) found that OSL ages from this region very often yield ages which are obviously way too old. These age overestimates were interpreted as a result of insufficient sediment bleaching. They also stated that it is impossible to correlate the periglacial surface below the uppermost diamict between different sites and that additional dates are needed. They also concluded that they did not favour either of the two existing models for deposition of the uppermost diamict unit ('Kyrkbacken till', 'Öresund diamict', 'Lund diamicton'); subglacial deposition as suggested by, e.g., Ringberg (2003) or deposition in a subaquatic setting (Malmberg Persson & Lagerlund 2003).

Larsen et al. (2009) agree in general with Houmark-Nielsen & Kjær's (2003) reconstruction but argue that from southern Sweden, little is known about older Baltic ice streams.

3 Study area and regional setting

The study area is situated in the very south of Sweden (Fig. 2). In the north, it starts in the southern outskirts of Malmö, and continues to the south coast. It spans from Falsterbo in the west to Smygehuk in the east. Data from outside that area have also been included in this study for comparison, but the interpretations are only valid for the study area itself.

The area can be divided into a mostly flat, slightly undulating part along the coasts and a hummocky part further inland (for more details on the morphological division see chapter 4.1.2).

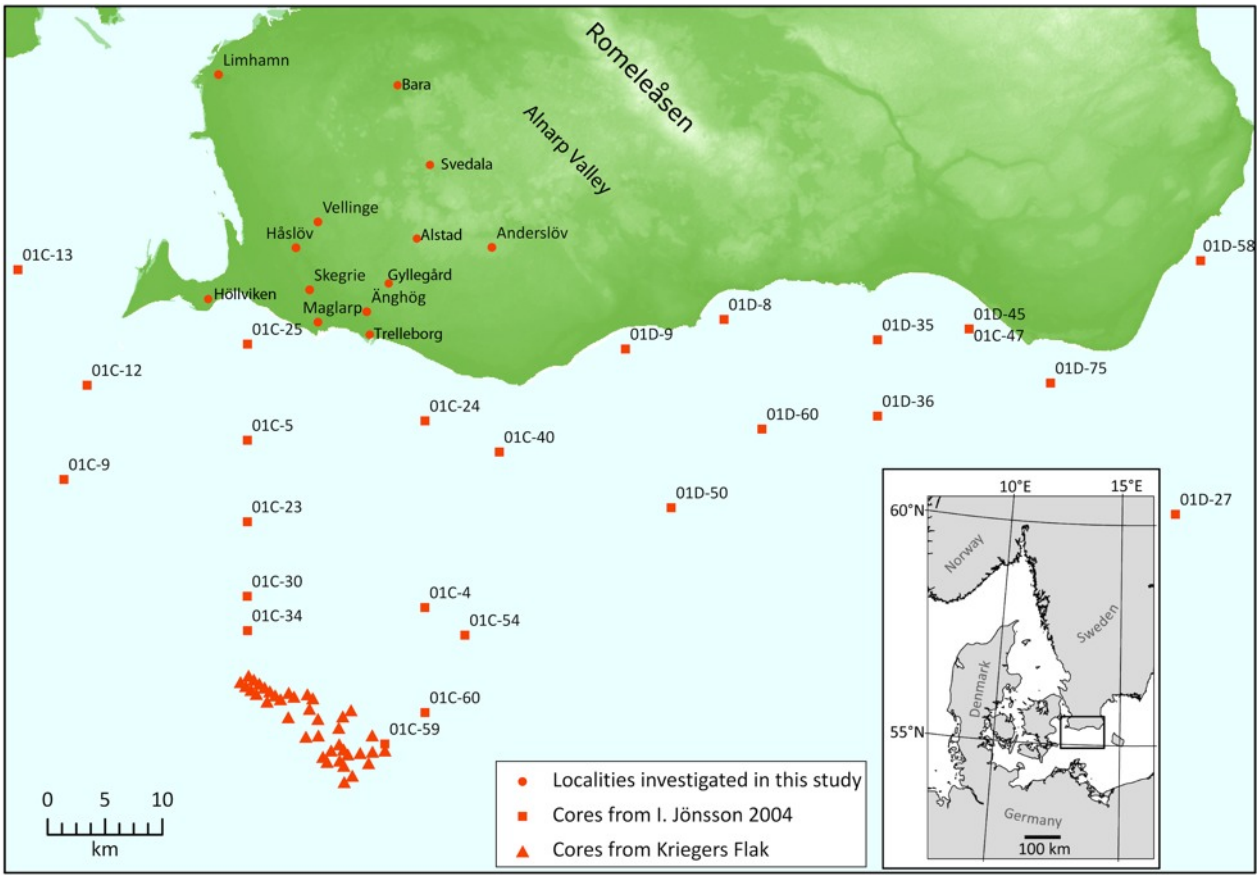

Fig. 2. Map showing southern Scania in the context of south-western Scandinavia and the data points mentioned in this study. Detailed investigation focussed on the area south-west of Romeleåsen.

4 Methods

4.1 Studies of existing data

4.1.1 Subsurface model

A model of the pre-Quaternary surface has been created by compiling existing drill logs from the Geological Survey of Sweden (SGU) well archive (Fig. 3). The model has then been validated with the information given in the geological maps of the area and their descriptions. The depth to bedrock in the logs is given in metres below surface and as the elevation of the reference point is often unknown, it needed to be reconstructed from a digital elevation model. Two such elevation models were tested for their suitability for the study area. One model provided by "Lantmäteriet" (the Swedish mapping authority) has been created from the elevation curves of existing maps and has a resolution of 50 m per pixel and a mean elevation error of 2.5 m. Small scale topography is omitted and step-shaped artefacts may be introduced in very flat areas. Another model uses data acquired by the Shuttle Radar Topography Mission (SRTM), acquired by radar interferometry; their quality has been controlled and improved by Jarvis et al. (2008). The resolution is 3 arc seconds (around 90 m at the equator) and the mean elevation error also around 2.5 m. They show a continuous picture of the surface but have considerable amounts of noise in very flat areas. It turned out that the SRTM-based elevation model is better suited to the purpose (due to its continuity) so the well logs were normalised to this model.

The well logs used for the modelling of the subsurface are not distributed equally over the map, they cluster around settlements and roads.

A reconstruction of the Quaternary units from the well logs has been attempted but was not very successful due to the greatly varying quality of the logs. As with all point data, a lot is left to interpolation and interpretation. Four profiles have been constructed to cover the investigated area (Fig. 4).

4.1.2 Geomorphological interpretation

A geomorphological interpretation of the SRTM-derived elevation model (DEM) has been carried out assisted by Quaternary geology maps Ae 23 (Trelleborg NV/Malmö SV, Ringberg 1975) and Ae 33 (Trelleborg NO, Daniel 1977), published by SGU.

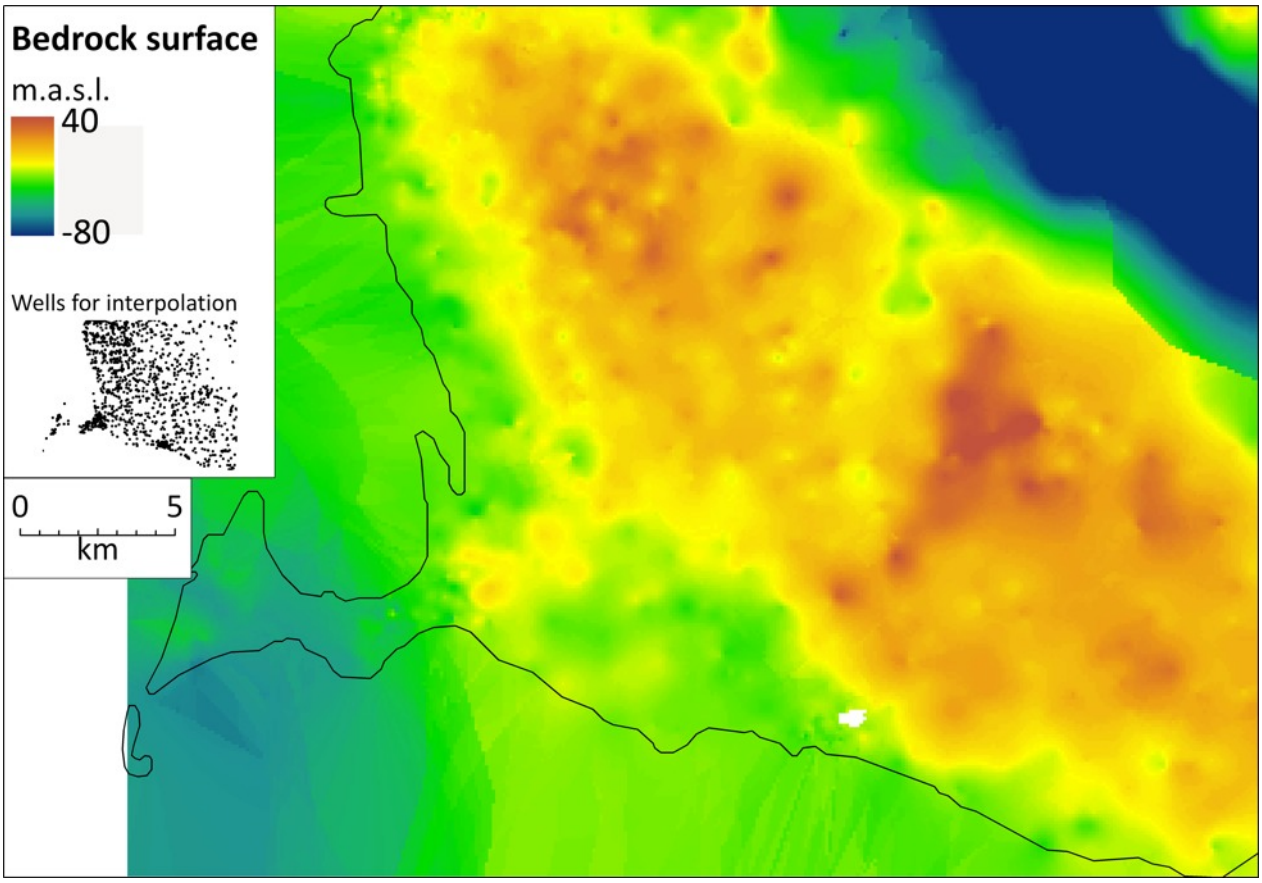

Fig. 3. A reconstruction of the surface of the pre-Quaternary bedrock in the study area based on well data. The map shows the result of an interpolation done with the 3D-Analyst of ArcMap using the "Kriging"-method, with SRTM-data used for calculation of m.a.s.l. The 1822 input-data-points are not distributed equally as can be seen from the inset map. The white spot is caused by a "No-Data" area in the DEM.

The interpretation concentrated on the coastal areas of south-western Scania and special focus was put on elongated landforms which could be indicative of ice movement in the area (Fig. 5).

4.2 Field investigations

Field work has been carried out in an approximately 4 m deep and around 200 m long ditch south of Vellinge (see Fig. 7). A 35 m long section has been selected due to some interesting deformations and drawn in a scale of 1:20 (Fig. 11, Appendix A, downsized).

The approximate level of the present surface was interpolated from values provided in a construction plan for points in the very near surroundings.

Five clast fabric measurements (of the clasts' a-axis) have been carried out in different units, each measurement consisting of at least 30 clasts (Evans & Benn 2004). Only clasts with an a-axis length between 20 and 60 mm and an a:b-ratio of at least 1.5:1 have been selected. The clast-fabric of the uppermost diamict unit has been measured on the opposite face of the ditch due to easier accessibility. The results of the clast-fabric measurements can be found in Fig. 9 and Appendix A.

Different parameters have been calculated to further help with the interpretation of the clast fabric. Those include the eigenvectors (V_1, V_2, V_3) and the normalized vector magnitudes (eigenvalues) S_1, S_2, S_3. V1 is parallel to the which describe the 'shape' and the strength of the fabric (Benn 1995). This shape (Fig. 13) varies between three end members (Benn 1994, 1995), the first being isotropic ($S_1 \sim S_2 \sim S_3$), the second one being girdle fabric ($S_1 \sim S_2 \gg S_3$), the third end member is cluster fabric ($S_1 \gg S_2 \sim S_3$).

4.3 Laboratory investigations

4.3.1 Grain size

The grain size distribution of samples from all units encountered during field work has been measured, the larger grains with sieves from 22.4–0.063 mm; the smaller grain sizes have been measured with hydrometers in sedimentation columns. The results from these measurements can be found in Appendix B.

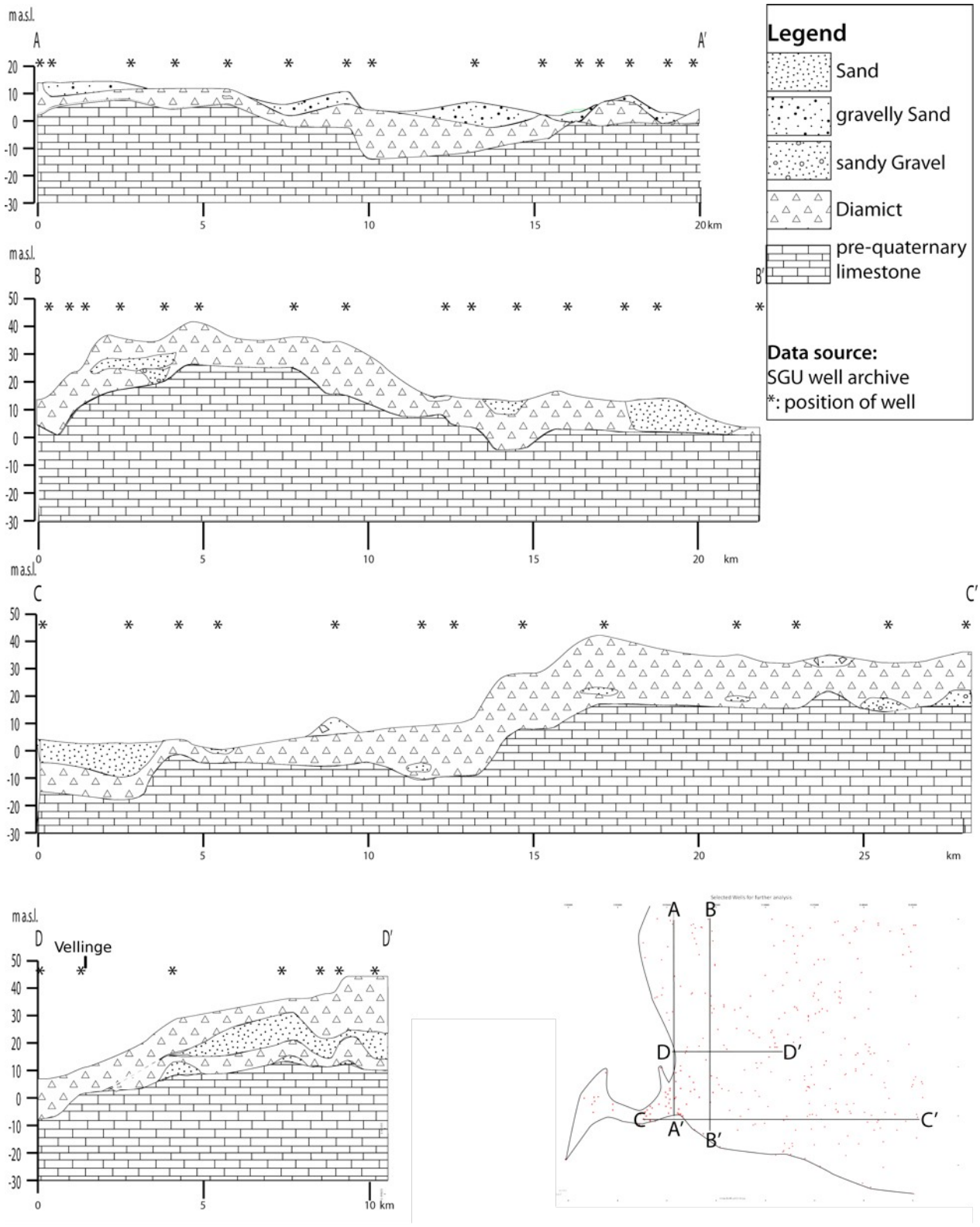

Fig. 4. The profiles have been drawn from data found in SGU's well archive and show the Quaternary deposits along the lines A to D.

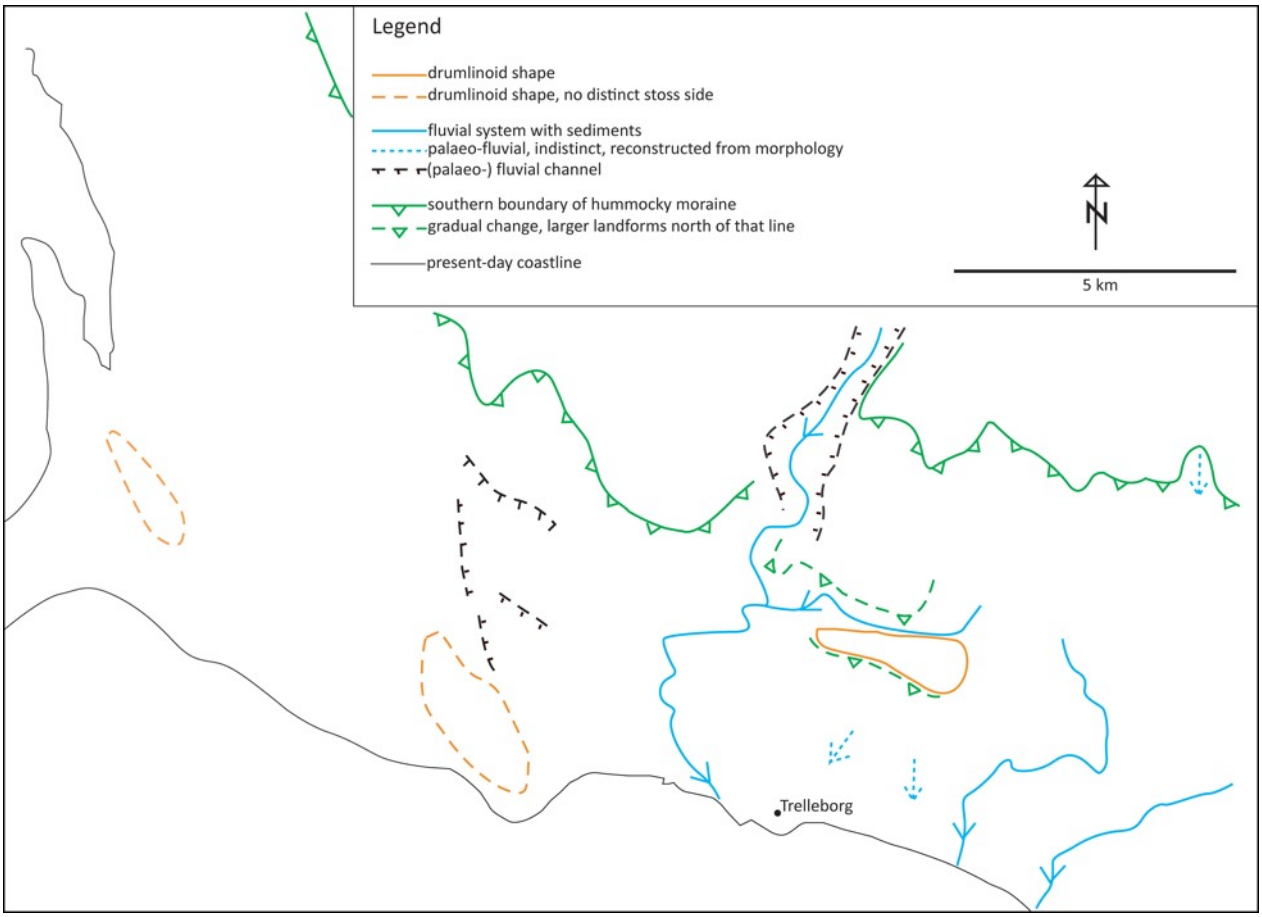

Fig. 5. Geomorphological overview of the study area, constructed from topographic maps and digital elevation models.

4.3.2 Provenance

To get an impression of the provenance of the different units, the fine gravel fraction has been analysed (Bridgland 1986; Evans & Benn 2004).

To compare results from different studies, it is important to count grains of the same size range, because the lithological composition changes significantly with grain size (Ehlers 1979). "Fine Gravel" has in this study been defined as grains between 2 and 5.6 mm which is almost in accordance with the size range used in the map descriptions by SGU. There a size range of 2–6 mm is used (Daniel 1977; Ringberg 1975, 1980).

Another problem with the comparison of different fine gravel studies is that almost every author sorts the lithology in differently defined classes. In this study, the clasts have been divided into 8 different classes; quartz, crystalline rocks, shale, sandstone, "fine sandstone", palaeozoic limestone, cretaceous/tertiary limestone, flint and others/unidentified.

To get a reliable result, it is necessary to count enough grains. An overview and discussion of the influence of different sample sizes on the standard errors for different frequencies of lithologies is given by Bridgland (1986). He reports results from a survey among researchers using fine gravel analysis, the mean sample size those researchers counted was *c.* 300 grains with a range from 50–1000. In this study, 309 grains were counted in the smallest sample and 756 in the largest one. From the tables in Appendix C it can be seen, that the percentage of lithologies that are present in larger proportions is much more stable than the ones that are only present in small numbers.

There are at least two different methods of displaying such data. One of these methods only uses one diagram, here all lithologies together sum up to 100% while the other method (Ehlers 1979) distinguishes between unstable (limestone) and stable lithologies (all other classes). The stable lithologies sum up to 100% and the amount of grains of unstable lithologies is given relative to the sum of stable grains. The first method is the one traditionally used in Sweden while the second one is more commonly used in Denmark and northern Germany. Both methods have advantages and disadvantages. The first method gives a quick overview but is influenced by the different weathering-susceptibility of different lithologies. The second method does not have this problem. There is a variant of the second method which plots the amounts

of the unstable grains not relative to the non calcareous lithologies but relative to the total number of grains. If the amount of flint and the amount of cretaceous-/tertiary limestone are compared, a rough guess about the degree of weathering is possible, because flint and the cretaceous-/tertiary limestone may come from the same source area. The samples investigated in this study had a very different depth to the (palaeo-) surface which might have lead to a different degree of weathering. This difference is also visible in the samples.

To keep the main text of this thesis short, the data are presented in the "Swedish" way, while the raw data and calculations after both methods are presented in Appendix C.

Fine gravel samples were also taken from sections in Håslöv, Skegrie, Maglarp, 'Änghög' and Anderslöv but as those samples showed strong signs of weathering they were not used for the reconstructions in this study. The results are, for reference, listed in Appendix C.

5 Results

5.1 Subsurface model

The pre-Quaternary bedrock (Fig. 3 is very close to the present ground surface in the study area. It is closest (at a depth of less than 1.5 m) along a NW-SE-trending line through Höllviken, sloping downwards NE and SW-ward of that line. The slope of that surface is gentle until it reaches a line Bara–Svedala where the slope increases strongly towards the Alnarp Valley. In this valley, the pre-Quaternary bedrock is at a level of more than 130 m below the present surface.

Relative to sea level, the bedrock surface has an elevation between *c.* -76 and *c.* +42 m in the investigated wells, being slightly below sea level along the coast line and reaching the highest elevations in the investigation area close to Alstad (Trelleborgs Kommun). Even if related to sea level, the Alnarp-valley is clearly visible in the interpolated map (Fig. 3) as a trough with steep walls.

In the borehole-data, it was possible to distinguish between bedrock, sorted sediments and diamict. It was however not possible to differentiate between different diamict units with a high reliability. Such a differentiation can in this case only be based on stratigraphical evidence, i.e. clearly recognisable beds of other sediments between two layers of diamict. Such indication has only been found in Profile D–D' (Fig. 4) where a thick layer of sand has been found to be between diamict in several boreholes.

5.2 Geomorphological interpretation

South-West Scania is characterized by two very different geomorphic regions, a flat landscape along the west and south coasts, and a hummocky landscape further inland (Fig. 5). The latter is described in more detail by Nilsson (1959). The boundary towards the hummocky moraine landscape as depicted in Fig. 5 does not exactly follow that proposed by Daniel (1977).

In the flat area, two of the three drumlinoid forms described for this area by Lidmar-Bergström et al. (1991) could be recognised in the DEM (in the western part of Fig. 5). Another drumlinoid landform has been identified close to the farm "Gyllegård", ca 3 km NE of Trelleborg. This landform is ca 3 km long, 0.8 km wide and 6 m high at the stoss side. The stoss side, pointing towards ESE, is much steeper than the lee side, and the landform is distinct and thus easily recognisable when contour lines with 1 m equidistance are drawn, showing a long axis trend WNW–ESE. This is in contrast to the landforms identified by Lidmar-Bergström et al. (1991) which trend NW–SE. Directly east of this drumlinoid landform close to Gyllegård there is a very flat area, slightly sloping to the east.

Other features that have been identified are the (relict) fluvial systems. Some of them have been found according to their sediments as reported in the geological map, while others are mainly reconstructed by their morphology if they produced valleys or valley like forms (Fig. 5). One distinct channel could be traced into the hummocky terrain, and another channel system in the flat terrain. The former channel trends NNE–SSW while the latter trends NW–SE (Fig. 5). The direction of the distinct channels as well as of the (relict) fluvial systems is towards the present coast.

6 Section in Vellinge

In the section in Vellinge (Fig. 7), three main units are exposed in a *c.* 200 m long and c. 4 m deep trench (Fig. 6). The contact with the pre-Quaternary surface is not exposed. The lowermost unit is a laterally continuous diamict with an undulating surface (Fig. 8). The middle unit consists of several synclines infilled by a succession of mainly fine grained clayey, silty and sandy sediments. Different types of deformation structures such as folding, thrusting and dewatering structures were seen in the sediments along the trench. The anticlines are cut by the uppermost unit which is a laterally continuous diamict. In some parts, the lowermost and the uppermost units are in direct erosive contact. One of the anticlines with its surrounding synclines was selected for a more detailed documentation of lithofacies, bed geometries and deformation structures (Fig. 11). The description follows a stratigraphic division based on three main units traced along the ditch, and a subdivision based on the detailed investigations. A composite lithostratigraphic log is presented in Fig. 9. Indicators for deformation are described separately from the units they occur in. The profile can be divided into three different units (chapters 6.1–6.3).

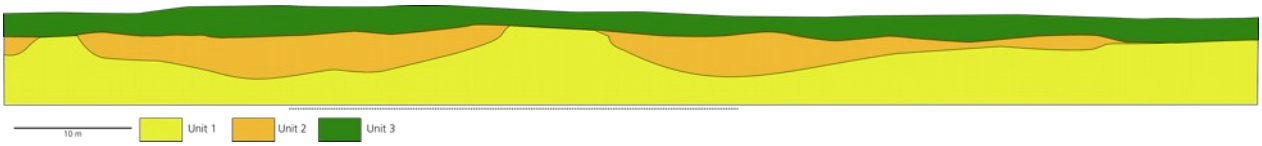

Fig. 6. Overview of the section in Vellinge. The dashed line shows the approximate position of the profile in Fig. 11.

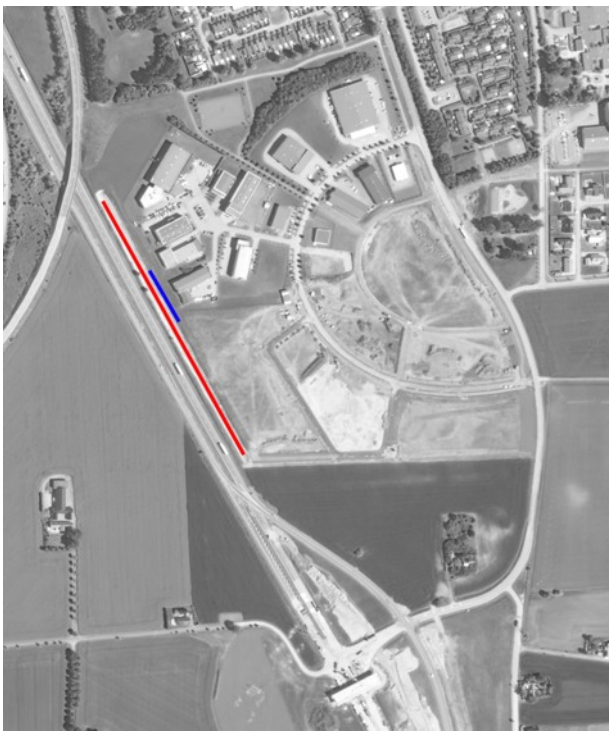

Fig. 7. The orthophoto shows the position of the section in the southern part of Vellinge. The red line depicts the total section while the blue line is the part documented in Fig. 9 and Appendix A. Photo ©Lantmäteriet 2010

Fig. 8. Sediment-filled synclines and cut anticlines. Photo: J. Anjar

6.1 Lower diamict (Unit 1)

Description The lowermost unit is at least 1.5 m thick (the lower boundary is not exposed) and continues laterally along the entire exposure. According to the reconstruction of the bedrock surface (Fig. 4, profile D), this unit probably continues to the pre-Quaternary surface situated a few m below the bottom of the ditch.

The upper boundary is undulating and is distinct (non-erosive) in the non-deformed parts and diffuse in the deformed parts. In the anticlines, the upper surface is erosive and in direct contact with the upper diamict.

This unit is a reddish grey , fine grained, massive, matrix supported diamict. According to field classification, the matrix has an uniform grain size, which according to laboratory analyses show a clay content of 15% and a silt content of 30–32% (Fig. 10). It contains many small clasts but clasts >5 cm are very rare (Fig. 12). The clasts are mainly angular to subangular (Fig. 10). Several cobble-sized clasts have short striae in different directions.

In the non-deformed part the diamict is homogeneous while in the uppermost deformed parts it is more heterogeneous. Some discolouration has been observed in the upper right part of the section, the discolouration is concentrated along fissures.

Three clast fabric measurements were carried out in this unit (Fig. 9, Appendix A). One shows a V1 strike/dip of 293° / 16° but an S_1 value of only 0.475. Fabric 4 is in contrast quite strong ($S_1 = 0.697$) and shows a direction of 145° / 17°. Fabric 5 is even stronger ($S_1 = 0.709$) and shows a SE-dipping first principal vector (133° / 21°).

Two samples from this unit were taken and analysed for the lithological composition of the fine-gravel fraction (Fig. 9, Appendix A). Those two samples contain high amounts of crystalline lithologies and palaeozoic as well as cretaceous / tertiary limestone. Their non-calcareous fraction differs mainly in the content of siltstone which is more as twice as high in sample VE1 than in sample VE2. The lithologies indicate a mixture of both local and far-travelled clasts. The amount of flint in both samples is similar as is the amount of cretaceous / tertiary limestone.

Interpretation The lower diamict is interpreted as a deformation till (Evans et al. 2006; Benn& Evans 2010) formed below in the deforming bed below an actively moving ice.

According to Benn (1994), deformation tills can be divided into two layers, often characterized by differences in clast fabric signatures. While such a lower layer of a

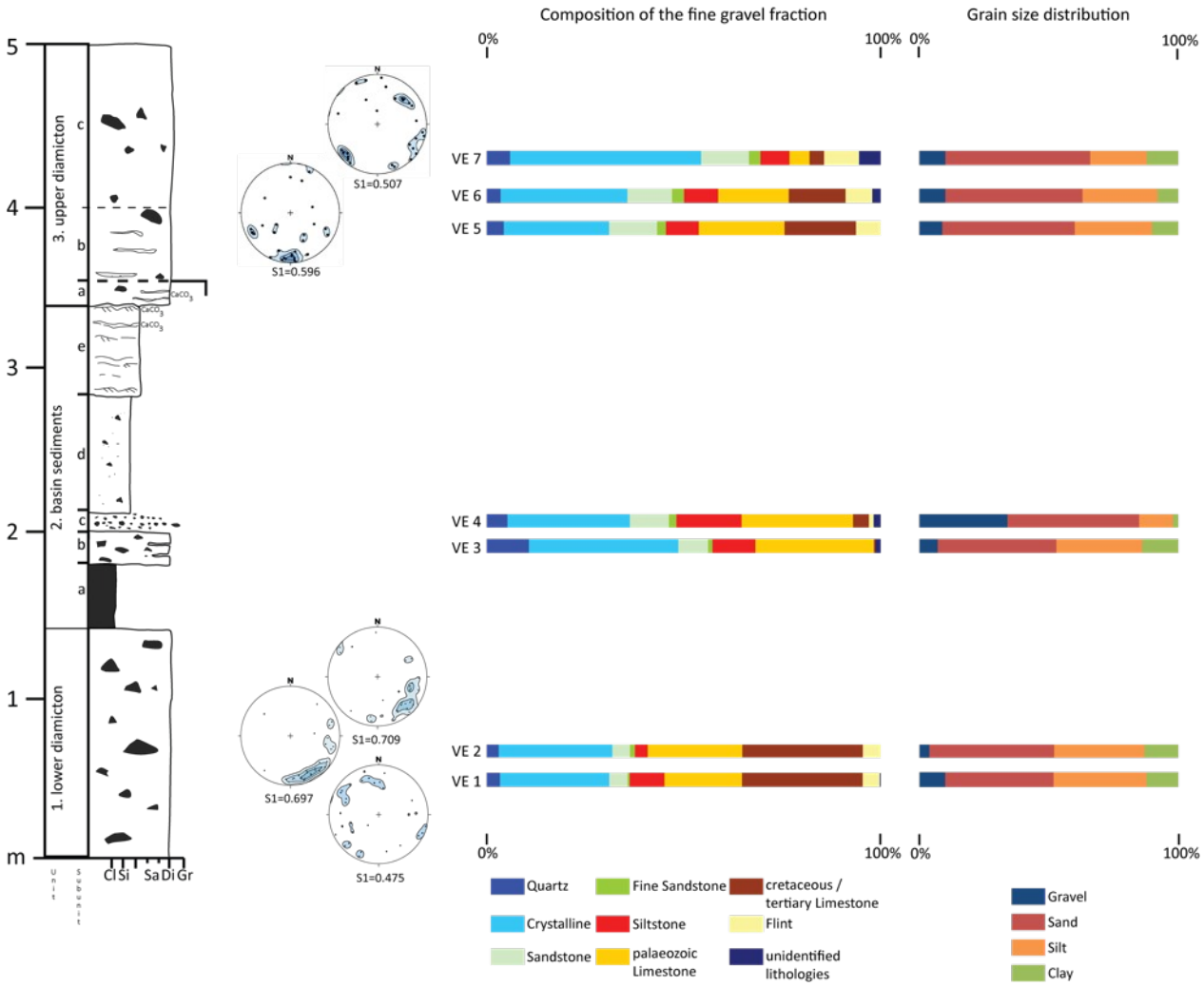

Fig. 9. A compilation of field and laboratory data for the section in Vellinge. Fine gravel data is plotted in the "Swedish" way. The grain size divisions follow DIN EN ISO 14689 (Deutsches Institut für Normung 2003).

deforming bed shows a very low degree of isotropy and a moderately elongated to elongated a-axis fabric with a maximum close to the former direction of ice flow, the upper layer has higher isotropy and a large variation in the elongation values. The fabrics F2 and F3 (Appendix A) show very low isotropy and an elongate a-axis fabric (Fig. 13), and could accordingly be assigned to the lower layer of a deforming bed. Their fabric maximum (V1) varies between 133° and 145°, indicating an ice flow direction from the south-east.

The diamict has a lateral continuity through the entire exposure and is very homogeneous (except in the vertically deformed parts at 22–32 m, Fig. 11) which are other indicators for a deformation till (McCarroll & Rijsdijk 2003; Benn & Evans 2010). The mixed lithologies indicate an interaction between the glacier and its bed, eroding the local bedrock and entraining it as debris in the deforming bed. The clasts have striae in different directions which is a sign for clast rotation and realignment during wear, and typical for the upper part of a deforming bed (Benn 1995; Benn & Evans 2010).

6.2 Basin sediments (Unit 2)

The sediments in the synclines can be divided into several subunits according to differences in lithofacies and sediment geometry (Appendix A).

The lower subunits (2a–2c) show distinct variations both in lateral and vertical directions. Their thickness and lateral distribution seems to follow the synclinal basins. The beds onlap in the slopes and the thickness increases towards the basin's deeper parts.

The upper subunits (2d–2e) have similar sedimentary properties along the whole ditch, and show a more continuous lateral distribution and a relatively constant thickness. The constant thickness of these subunits is only interrupted at the truncated tops of the anticlines.

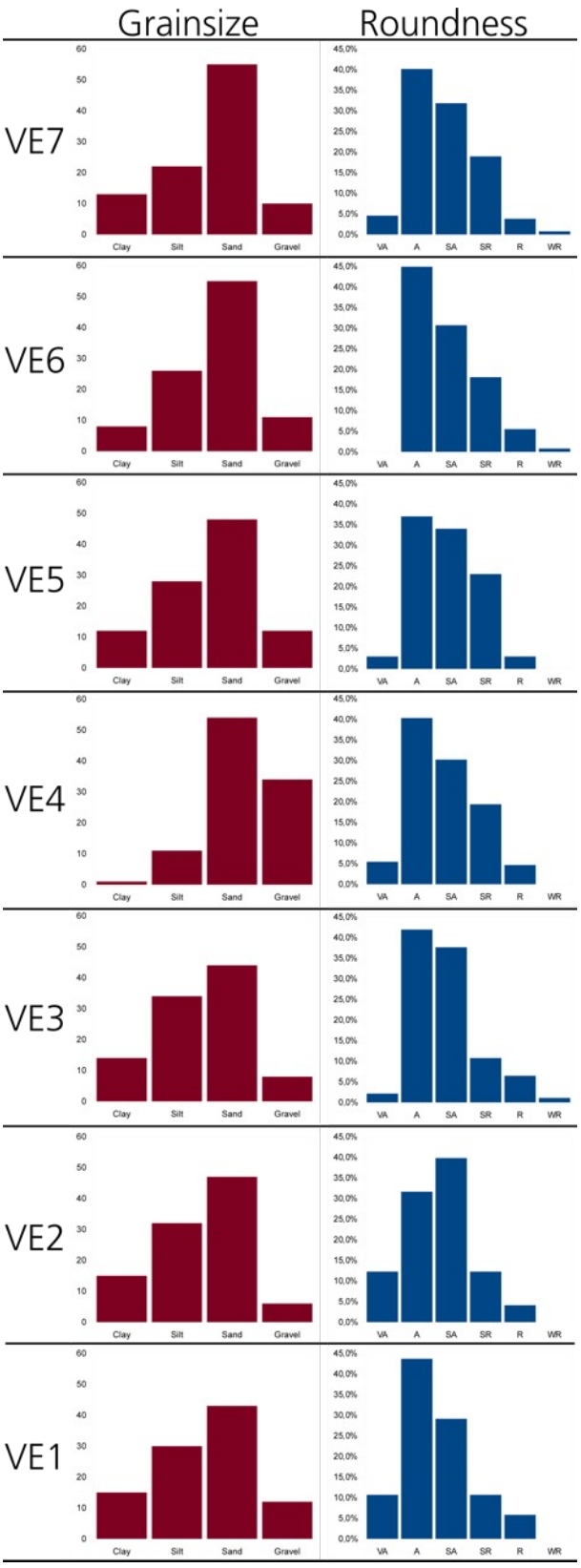

Fig. 10. Grain size distribution and roundness in the 5.6–8 mm size range of the different samples (cf. Fig. 9)

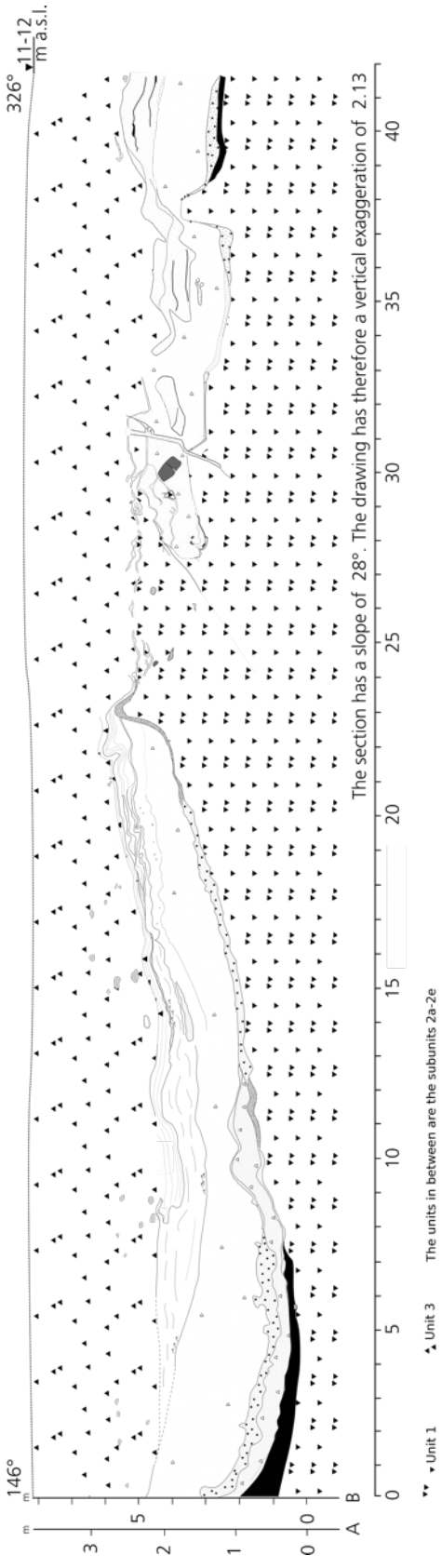

Fig. 11. The section in Vellinge. Vertical scale A is corrected for the slope, B is like it was measured in the field. A larger version can be found in Appendix A

Fig. 12. Representative picture of the lower diamict (described in chapter 6.1). Photo: L. Adrielsson

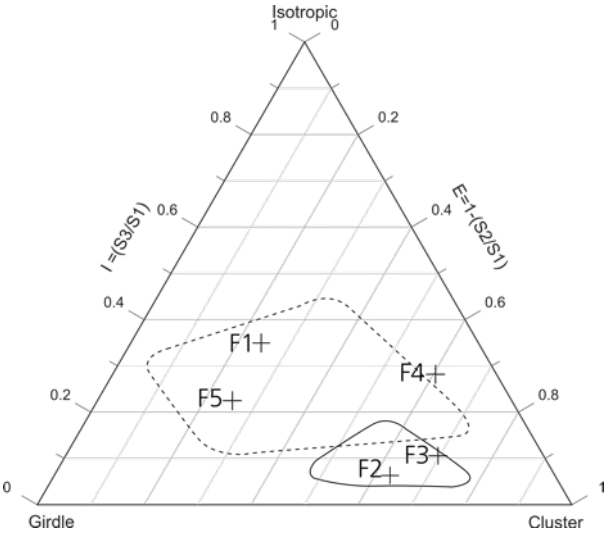

Fig. 13. A-axis-fabrics for the section in Vellinge. The field with dashed line shows possible values for the upper layer of a deformation till, the field with solid line values for the lower layer (Dowdeswell & Sharp 1986, cited after Benn 1994) For sampling localities see Appendix A, for an explanatory key to this type of diagram, see Benn (1994).

6.2.1 Clay (Subunit 2a)

Description This subunit consists of a dark grey, massive clay. The contact to the lower diamict is conformable. In the left part of the section, the maximum thickness of the clay reaches *c.* 30 cm, the thickness decreases towards the basin slope and the subunit finally tapers out. In the upper part, thin beds of diamict (1–3 cm) are intercalated with the clay, resulting in an interfingering contact with Subunit 2b.

Interpretation This clay has been deposited by settling from suspension. Deposition of suspended clay occurs in standing water bodies. Its massive appearance shows a continuous deposition without periodical interruptions or sediment pulses.

6.2.2 Middle diamict (Subunit 2b)

Description This subunit is *c.* 20 cm thick and consists of grey, matrix-supported diamict. The diamict is massive to diffusely stratified. Thin beds of diamict are separated by very thin, diffuse and discontinuous sand beds.

The upper boundary of the subunit is irregularly undulating and the transition to Subunit 2c seems to be gradual or interfingering. At 7.5–13 m (Fig. 11, Appendix. A), the clay of Subunit 2a is missing and the diamict beds are directly over- and underlain by sand and gravel from Subunit 2c.

The matrix of this unit has a similar grain size distribution as Unit 1. In one sample, 14% clay and 34% silt have been measured. Angular and subangular clasts dominate the 5.6–8 mm fraction (Fig. 10).

The fine gravel fraction of one sample (VE3) has been analysed for its lithological composition (Fig. 9). It contains almost 30% palaeozoic limestone (far-travelled) but no local cretaceous / tertiary limestone. The sample also contains more than 10% siltstone which is another far travelled erratic.

Interpretation This diamict is interpreted as being the result of sediment gravity flows. The material also contains much silt and clay, indicating that the flows have been cohesive (Fig. 9) and had a high density as is shown by the presence of gravel-sized clasts which have been buoyantly uplifted (Mulder & Alexander 2001). The diffuse sand beds that are separating the diamict beds indicate a succession of different debris flows.

The lithological composition is significantly different from the one of unit 1, so a reworking of sediments of unit 1 can be excluded. A direct melt out of debris from ice is thus a likely source of the material.

6.2.3 Sand and gravel (Subunit 2c)

Description On top of the middle diamict subunit and in places below the clay (Subunit 2a), another subunit of crudely bedded sediments is found.

The upper and lower boundaries are irregularly deformed, and it can be traced through large parts of the section (Fig. 11, Appendix A) and has a thickness varying between a few cm and 20 cm.

It consists of coarse sand and gravel beds with massive structure. The degree of sorting is variable and frequent transitions from sandy to gravelly beds occur. Some of the beds have during field work been classified as diamict. One sample from the left part of this subunit (VE4, Ap-

pendix A) shows a silt content of 11%; 54% sand and 34% gravel and is thus classified as gravelly sand. The 5.6–8 mm fraction of this sample is dominated by angular and subangular clasts but contains also *c.* 20% of subrounded clasts (Fig. 10).

One sample (VE4) has been analysed for the lithological composition of its fine gravel fraction (Fig. 9). The stable lithologies consist to almost 25% of siltstone and shale, while the flint content is less than 2%. In the calcareous part, this relation between far-travelled and local lithologies is also reflected by almost 30% far-travelled palaeozoic limestone but only 4% local cretaceous / tertiary limestone.

Interpretation This subunit has a very similar lithological composition as Subunit 2b, the main difference between them is the higher degree of sorting in Subunit 2c. This subunit is therefore interpreted as deposition from bedload transport in small, temporary streams. The transport could also have occured in a hyperconcentrated density flow (grain flow, Mulder & Alexander 2001)

According to the clast roundness and the degree of sorting, the transport distance has been short.

6.2.4 Massive sandy silt (Subunit 2d)

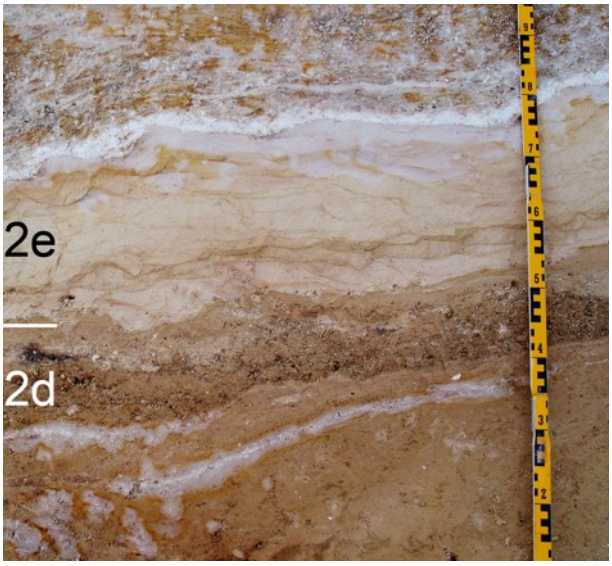

Fig. 14. Subunit 2d in the lower part of the picture. Diamictic part at the 4–5 dm mark. Subunit 2e starts above the diamictic part of Subunit 2d. On the top, 2e is draped by calcite. Photo contrast adjusted. Photo: L. Adrielsson

Description This subunit is *c.* 1 m thick (Fig. 11) and has a massive structure. The predominant grain sizes are coarse silt and fine sand (as determined in the field) .

The sediment is generally poor in coarse clasts but granules and small pebbles made of porous limestone are regularly scattered within the massive matrix which gives a white-spotted appearance. The content of granule-sized clasts slightly increases upwards so that the appearance is more diamictic in the uppermost part. In the upper part of the small basin at 10–19 m (Fig. 11), the sediment is classified as a diamict with a few small lenses of gravelly sand (Fig. 14).

Interpretation This subunit is interpreted as either a debris flow or a hyperconcentrated, muddy density flow (Mulder & Alexander 2001).

According to Hjulström's diagram (Selley 1976, p.172), fine sand and silt are deposited at flow velocities below *c.* 4–5 cm/s. This flow velocity would however be too low to transport granules and small pebbles in water. It is thus likely that the flow had a higher density, i.e. that it was loaded with sediments and could therefore transport the larger clasts.

For the larger clasts (which almost exclusively consist of porous limestone) there are several possible origins. One explanation is that the larger clasts have the same origin as the matrix surrounding them and that the porous limestone was concentrated relative to the other lithologies due to its low density. Another possible explanation for the larger clasts is that they did not come from the same source as the matrix. But in that case it is difficult to explain why they are almost exclusively of cretaceous / tertiary origin and do not contain a significant proportion of other lithologies.

6.2.5 Stratified sand and silt (Subunit 2e)

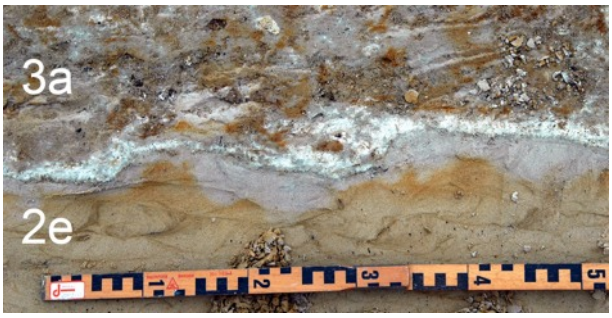

Fig. 15. Calcite draping on the upper boundary of Subunit 2e.

Description This subunit consists of *c.* 0.5 m of distinctly stratified fine sand and silt with a rapid transition from Subunit 2d. The contact is sharp but non-erosive.

The fine sand is ripple-laminated while the silty beds exhibit planar lamination. In the upper part of the laminated sediments, cm-thick beds of calcite are interbed-

ded. In some places, the white deposits are draped on the ripple-laminated sand (Fig. 14).

Interpretation This subunit was deposited by stream flow, creating the ripple laminations. To create ripple bedforms in fine sand and coarse silt, a flow velocity of *c.* 20 cm/s is needed (Leeder 1982, p. 85). The beds of laminated silt suggest a non-steady flow with varying velocities. During phases of decreased flow velocity, silt fallout from suspension increased.

The calcite has been precipitated from an oversaturated aqueous solution. This can either happen if the water pressure decreases or if the concentration of the solutes increase (Hallet 1976). The water pressure decreases if pressurized water exits a confined space, i.e. if it enters a subglacial cavity or if it flows out at the front of the glacier. During freezing of $CaCO_3$-solutions, the content in Ca^{2+}-ions is much lower in the ice than in the water as freezing experiments by Hallet (1976) have shown. This implies that the content of Ca^{2+}-ions increases in the subglacial melt water during refreezing at the glacier sole. If the saturation point is exceeded, $CaCO_3$ is precipitated. The calcite beds thus represent events during which the saturation concentration in the water was exceeded. As more than one such bed exists, these conditions occurred repeatedly.

6.3 Upper diamict (Unit 3)

This diamict is divided into three subunits (Fig. 9); a stratified lower part with cm-thick beds of calcite (Subunit 3a), a massive matrix-supported part with smudges and some small intraclasts of laminated fine sand (Subunit 3b) and an upper, more homogeneous part (Subunit 3c). The two lower subunits are separated by an erosive contact which could be traced along the entire section. Samples for further analysis and fabric measurements have been taken in Subunit 3c.

6.3.1 Stratified diamict (Subunit 3a)

Description This subunit has a stratified appearance and contains both diamictic as well as cm-thick calcite and thin fine-sand beds (Fig. 9). The subunit is most prominent between 11 and 24 m (Fig. 11) where it is *c.* 20 cm thick. It is difficult to trace this subunit between 25 and 32 m. Its lower boundary to unit 2 is sharp and the upper boundary to Subunit 3b is erosive.

Interpretation This subunit can either be interpreted as the result of subaqueous (cohesive) debris flows, or possibly as subglacial till. The sediments are of similar appearance to the uppermost stratified sand but with an addition of diamict beds and a decrease and thinning of sand beds.

One strong indication for a deposition of subunit 3a as debris flows are the preserved primary sedimentary structures in Subunit 2e. They would probably have been destroyed in a deforming bed where the uppermost 0.5 m account for 80–90% of the movement of the glacier (Boulton & Hindmarsh 1987). Subglacial deposition can thus either occur below a glacier decoupled from its bed (Boulton et al. 2001) or by sliding over a frozen bed. While many researchers propose that such a glacier movement without bed deformation could also happen if the bed is frozen, Waller (2001) states that even frozen beds can be deformed by a glacier moving over them. The most likely explanation for subglacial deposition is thus deposition by a decoupled glacier.

6.3.2 Diamict with smudges and boudins (Subunit 3b)

Description This subunit is a massive, matrix supported, clast-poor diamict. It contains deformed inclusions of calcite as well as intraclasts of laminated fine sand (Fig. 9). The boundary to Subunit 3a is in parts distinct and erosive while other parts are more diffuse and undulating. It was not possible to trace this subunit between 25 and 32 m (Fig. 11). The boundary towards Subunit 3c is gradual.

One fabric measurement (F4) was taken in this subunit at around 20 cm above the lower boundary (on the opposite side of the ditch, Appendix A). This measurement revealed a V1-vector of 185° / 17° with a strength of S_1=0.596.

Interpretation This subunit is interpreted as subglacial deformation till. The erosive lower boundary of Subunit 3b implies that the active ice had direct contact with the bed and that the deposition was preceded by basal erosion.

During erosion, sediment rafts were picked up from Subunit 2d. The fine sand intraclasts form boudinage structures indicative for simple shear in a deforming bed (McCarroll & Rijsdijk 2003). The homogenisation of the deforming bed is not complete, as the presence of distinct rafts shows.

The isotropy value of the fabric measured in this unit is around 0.3 (Fig. 13), i.e. much higher than the fabrics measured in unit 1. This could be indicative for this till representing an upper layer of a deformation bed (Benn 1994). The fabric is still quite elongate which implies that the clasts were free to rotate so they could become parallel with the principal axis of extensional strain (Benn & Evans 2010). The clast rotation is best explained by the March theory (Hooyer & Iverson 2000), which results in strong fabrics regardless of the initial orientation and the aspect ratios of the clasts.

The lateral continuity through the entire section (Fig. 11) is another indicator for the interpretation as a subglacial deformation till. The mixture of both local lithologies as well as far-travelled erratics can be interpreted as a

sign of erosion of the substratum by the glacier. The lithological composition seems to represent a mixing of unit 1 and unit 2, showing that both those units were eroded.

6.3.3 Homogeneous diamict (Subunit 3c)

Description This subunit is *c.* 1 m thick and can be traced along the whole section (Fig. 11). Its lower boundary is gradual and the upper boundary represents the present ground surface. This subunit has a homogeneous appearance throughout all its extent.

The diamict has a clayey, silty to fine sandy matrix and contains *c.* 10% clay, up to 28% silt and up to 55% sand (Fig. 10). The sand is mainly fine sand (Appendix B). The 5.6–8 mm fraction contains a high proportion of angular and subangular clasts, while the lowermost sample from this subunit (VE5, Fig. 10) shows a relatively higher proportion of subrounded clasts.

One fabric measurement (F5) was carried out in this subunit (Fig. 9, measured on the opposite (eastern) side of the ditch). The measurement was taken at around 90 cm below the present surface (Appendix A). It shows a V1 strike/dip of 52° / 12° and a fabric strength of only 0.507.

The fine gravel fraction of this unit has been analysed for its lithological composition in three samples (VE5, VE6, VE7, Fig. 9). The proportion of flint is approximately the same in all three samples. Samples VE5 and VE6 contain a substantial amount of both far-travelled palaeozoic as well as local cretaceous-tertiary limestone while the limestone content is much lower in the uppermost sample.

Interpretation This subunit is interpreted as subglacial deformation till with post-depositional modification in its upper parts.

The gradual transition to Subunit 3b is indicative for a continuous sedimentary process. This subunit does not contain visible sediment rafts from the lower (sub-) units, which means a more complete homogenisation due to a higher strain rate.

The isotropy value of the clast fabric is less than that for the underlaying Subunit 3b, much less elongate and has a girdle shape (Fig. 13), which is also supported by the lower strength. The low strength and the girdle shape can, however, be due to post-depositional frost processes, as such low elongation is not typical for a subglacial deformation till (Benn 1994).

The limestone content of Subunit 3c is much lower than in the samples from Subunit 3b, while the other lithologies have approximately the same abundance in both subunits. As the limestones are easily weathered, this difference could be due to post-depositional solution of the carbonate. This interpretation is based on the similar proportion of flint in all three samples from unit 3 (VE5,VE6,VE7, Fig. 9).

Fig. 16. Flow folds on top of Unit 2e. Picture taken at *c.* 20 m. Lens cap has 67mm diameter.

6.4 Deformation structures

Description The deformational structures in this section can be described according to their type and to their relative size, as suggested by McCarroll & Rijsdijk (2003) and Van der Wateren et al. (2000) .

The largest structures visible in the section are the synforms and the (mostly eroded) antiforms which can be traced along the entire ditch (Fig. 6). The inclinations of the bedding planes in unit 2 have been steepened and follow the synforms and antiforms.

Two diapirs protruding from unit 1 are present in the investigated part of the section (Fig. 11), one at 23–24 m and one at 37–39 m. The diapir at 23–24 m is a few dm high and covered by the material from Subunit 2c. The diapir at 37–39 m is around 2 m high and is not covered by gravelly sand on its top but only on its flanks. The sediment cover of this diapir thickens away from the diapir.

Subunit 2e shows distinct flow folds (Fig. 16, classified according to McCarroll & Rijsdijk 2003) in its uppermost part (at 18–23 m, Fig. 11). Some of these folds are asymmetrical and some are imbricated (at *c.* 20 m, Fig. 11). Their axial planes are dipping towards a northern direction. At *c.*21 m, the folds are open folds. In the lowermost part of the syncline infillings, Subunit 2c shows an irregular thickening in the lowermost part of the basin (at 5–8 m, Fig. 11) while the subunit is much thinner in the slope. Such a thickening could, according to McCarroll & Rijsdijk (2003), be classified as sags into Subunit 2b and diapirs into Subunit 2c.

The uppermost part of Subunit 2e is pulled out northwards at 8–9 m (Fig. 11) and forms a distinct tongue in Subunit 3a.

There are two kinds of deformations containing intraclasts of sorted sediments. Unit 1 contains isolated, quite circular balls and pillows of sorted sediments which probably originate from Subunit 2c and can be interpreted as "sunken" load casts. (Fig. 17). Unit 3b also contains intraclasts but here, the material has large similarities with

Fig. 17. Intraclast of gravelly sand in the lowermost diamict. Picture taken at *c.* 25 m along the section.

the material from Subunit 2d. The sediment rafts in Unit 3b are attenuated and are diffuse smudges and boudinage-structures (McCarroll & Rijsdijk 2003). The clastic dyke at *c.* 30 m (Fig. 11, Fig. 18) originates as a very narrow fissure in unit 1. It widens upwards and has its upper end at the lower boundary of unit 3. It is filled with massive, poorly sorted gravelly sand and contains scattered, pebble sized clasts. The contact to unit 2 is sharp. The clastic dyke is dipping towards the south.

Fig. 18. Clastic dyke. Picture taken at *c.* 30 m along the section. Photo: J. Anjar

Interpretation The synclines and anticlines (Fig. 6) are the result of horizontal compression. Such compression can be the result of buckling in the proglacial environment (Croot 1988). Compression can also occur on slopes induced by gravity (McCarroll & Rijsdijk 2003) but the flat landscape does not support that interpretation. It is thus more likely that the compression was induced by a pushing, advancing glacier. The décollement plane is not visible and must thus be located somewhere beneath the section, one likely location for that plane is at the boundary between the diamict and the bedrock.

The overturned folds in the uppermost part of unit 2 at 18–23 m (Fig. 11) are formed by simple shear. The folds are related to the basin (their axial planes dip towards the north) and were probably formed due to gravity-induced shear stresses along a depositional slope. This thus indicates sediment flow down a basin slope towards the south, which is opposite to the ice movement direction and thus excludes deformation by moving ice (McCarroll & Rijsdijk 2003).

Unit 1 shows features such as diapirs, large upwelling structures (e.g. the one between *c.* 20–30 m, Fig. 11) and intraclasts , features that only can form if the unit is fluidized. Diapirs are formed due to density differences, i.e. when sediments of lower density move upward into sediments of higher density (Leeder 1982, p. 114). This process of density inversion (and the resulting instability) was probably induced by the addition of pressurized pore water from below. Such increase in water content can result in both lowering of the density and the yield strength of the diamict. The sandy gravelly intraclasts in unit 1 must thus have sunk to their present position when the diamict was fluidized, due to a difference in density (McCarroll & Rijsdijk 2003).

Clastic dykes are sediment-filled, more or less vertical crevasses and can form in different ways, either by downward injection of sediments (Le Heron & Etienne 2005) or by upward infill of hydrofractures (Rijsdijk et al. 1999).

Downward injection can occur if a glacier advances over stratified deposits (Boulton & Caban 1995). Clastic dykes can form from below in settings with a confined aquifer below the glacier, where an advance of the glacier induces a high pressure gradient and an upward groundwater flow. This flow widens pre-existing fault planes in the aquiclude which are subsequently filled with sediment from the aquifer (Rijsdijk et al. 1999). The aquiclude can either be permafrost (Boulton & Caban 1995) or a sedimentary layer with low permeability (Rijsdijk et al. 1999). The clastic dyke (Fig. 18) at 28–31 m (Fig. 11) is rooted in the upper part of unit 1 and cuts through the sediments of unit 2. Thus an injection from below is the likely type of formation for the dyke, suggesting a confined aquifer below an advancing glacier. The event of hydrofracturing must be younger than Subunit 2d.

The gravel and sand pillows (Fig. 17) in the uppermost part of unit 1 (at *c.* 20–30 m, Fig. 11) are interpreted as load casts (McCarroll & Rijsdijk 2003), which are caused by density inversion and driven by gravity. The density difference was increased by the addition of water to unit 1, decreasing its density. The pillows formed when denser sediment from unit 2 sunk into a liquified part of the unit 1 diamict. The sand and gravel pillows are totally detached from their host sediment and their primary bedding was completely destroyed.

Also the deformed bedding planes of subunits 2b–2d are interpreted as load casts (McCarroll & Rijsdijk 2003). They were most probably water-saturated, and thus reduced in strength. This loss of strength with subsequent fluidization can either have been induced by an increase in pore water pressure or by external disturbance. Pore water pressure can be increased by addition of sediments on the top. External disturbance can ,e.g., be triggered by the rise of the anticlines or by the formation of diapirs.

Another indicator for deformation was not observed directly in the section but was revealed by fabric analysis. One of the fabric measurements (F1, Appendix A) is much weaker than the others (F2, F3) from this unit. The orientation is much more scattered, which suggests reorientation of clasts during deposition. Reorientation can not occur in a solid diamict but requires a liquified sediment.

7 Depositional environment reconstruction

The depositional processes and the post-depositional deformation for the sediment succession in Vellinge (Fig. 11) are interpreted to represent two glacial advances with a phase of deglaciation in between. A model of the glacial history is presented in four stages as shown in Fig. 19.

7.1 Stage I: A Baltic ice stream

The unit 1 diamict is interpreted as a deformation till representing subglacial conditions beneath an active glacier. The deformation till indicates a coupling between the glacier and its bed, with the bed deforming due to subglacial shear.

Deformation occurs when induced stresses exceed the yield strength of the diamict (Benn & Evans 2010, p. 114), while different models exist on the behaviour of till for stresses above the yield strength.

Water below a glacier can either flow in a distributed way (e.g. as pore water within the deforming bed) or in channels (Willis 1995). As no sand lenses or channel infills were found in unit 1, there is no indication for a channelized drainage. Thus a porous, distributed flow in the deforming bed is more likely.

The strength of the diamict can be decreased by an increased pore water pressure. If the strength is decreased, the response of the sediment to applied stress is increased. Boulton et al. (2001) concluded that the balance between basal sliding and bed deformation is determined by the degree of coupling of the glacier to the bed. This coupling, in turn, is governed by fluctuations in water pressure beneath the glacier. Boulton et al. (2001) suggested that undrained sediments can be a product of rapidly advancing glaciers and that the pressure can change rapidly.

This increased pore water pressure beneath the glacier has several effects, it not only decreases the strength of the diamict but it decreases the effect of bed roughness (Benn & Evans 2010) and concentrates the stresses on that spots of the bed that are still in direct contact with the ice. This stress concentration increases the amount of sliding (Willis 1995). This means that the effects keep each other in balance.

An increase in ice velocity can, if the discharge of ice is faster than the ice formation upstream lead to a decrease in ice thickness (Paterson 1994; Benn & Evans 2010) and would thus support the model of a thin ice in the area (Ringberg 2003).

The lithological composition of unit 1 shows a mixture of local and far-travelled clasts. The high contents of cretaceous / tertiary limestone suggest erosion by the glacier by means of interaction with the local bedrock (Fig. 20) in an upstream direction. As indicated from the lithologic composition of the Unit 1 diamict, the subglacial transport in a deforming bed was long enough to create a homogeneous mixture of local and far-travelled lithologies. As the lower boundary of unit 1 was not exposed, it is, however, not known if there is an erosive contact with the bedrock at the site.

According to the fabric measurements (F2 and F3, Appendix A), the ice-flow direction was from the south-east. The content of palaeozoic limestone and siltstone indicate a Baltic provenance. The high ice velocities, as indicated from the deforming bed sedimentsand thin ice suggest ice-stream conditions (Truffer & Echelmeyer 2003).

7.2 Stage II: Ice stagnation and dead-ice melting

The sediments in subunits 2a-2c are interpreted to represent infilling of small basins with lacustrine sediments (Subunit 2a), terrestrial debris flow diamict (Fig. 19, stage II A), subaqueous debris flows (Fig. 19, stage II B) and stream deposits (Subunits 2b-2c).

Several different environments are possible for the infilling of basins by gravity driven processes. They occur either in paraglacial environments (Slaymaker 2009) where unstable slopes are brought to more stable conditions by gravity or in small basins in a disintegrating dead-ice environment where debris melts out from the ice or in subglacial cavities.

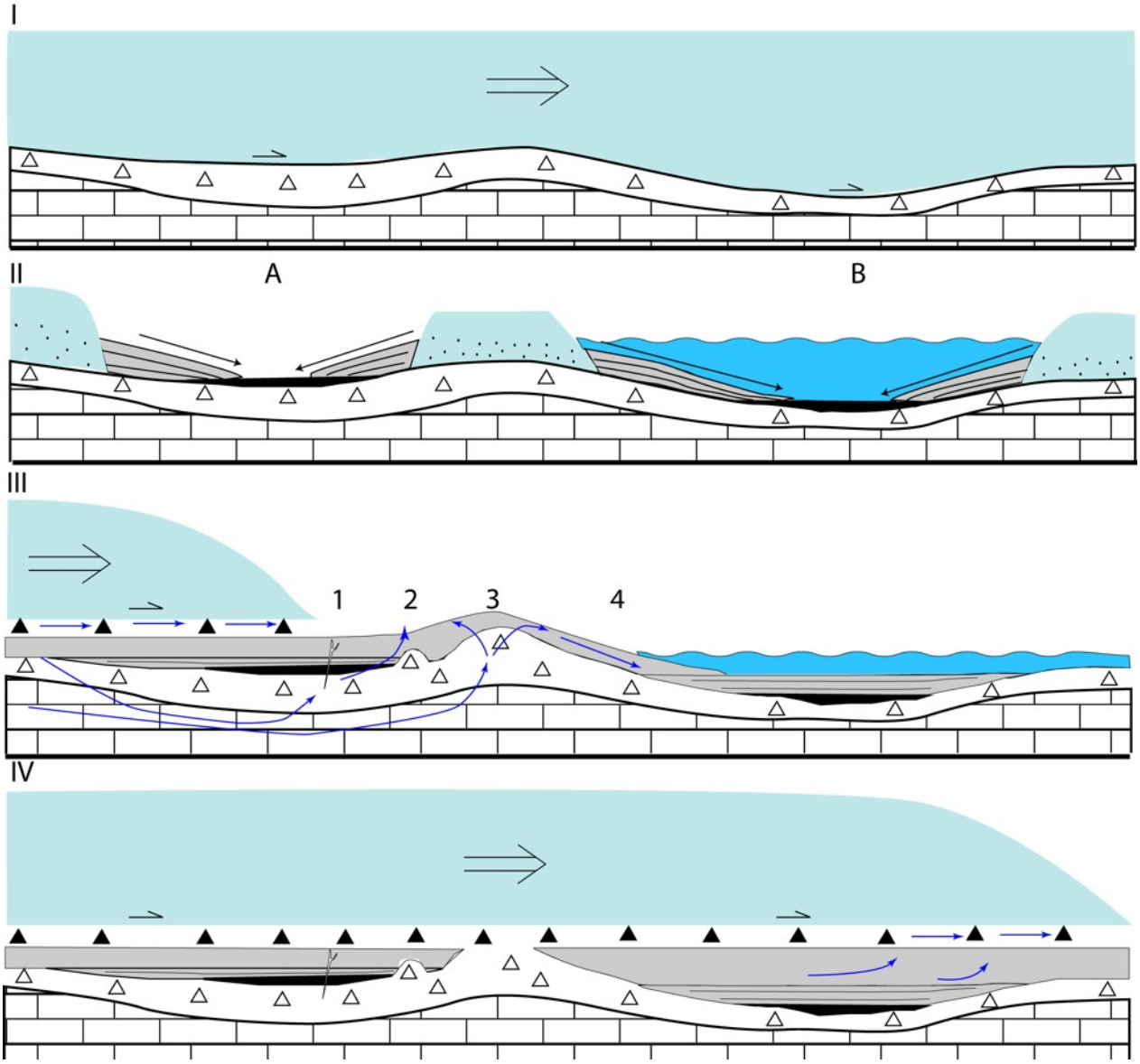

Fig. 19. Depositional model for the section in Vellinge. Light blue: ice, dark blue: water, hollow triangles: unit 1, black and grey: unit 2, solid triangles: unit 3

The interpretation of the depositional history during this stage is mainly based on the lithological composition and properties of the sediments in comparison to the lower till.

Deposition needs a debris source. The lithological composition of the subunits 2b and 2c differs significantly from the lower till, mainly in that they contain virtually no local lithologies. A gravitational reworking of material from unit 1 is thus an unlikely source for these subunits.

Indication for deposition in a disintegrating dead-ice environment is given by the composition where only the far-travelled lithologies are present but the local debris is missing. This can take place as deposition from melt-out from the upper parts of stagnant ice, followed by gravitational reworking of that material into small basins between the remaining dead-ice.

Deposition of subunits 2a–2c in subglacial cavities would require a decoupling of the ice and its bed. This is unlikely as indicators for periodic coupling (and shearing) under an active ice area absent. In such an environment, the possibility of outsized clasts falling from the cavity ceiling would have been high, but no such clasts were observed in Subunit 2a. This makes a deposition in a subglacial environment unlikely. A subglacial environment could, however be an explanation for the encountered fine-gravel clasts in Subunit 2d (discussed in more detail in stage III) but does not explain the selection of low-density lithologies.

As the clast lithology of Subunits 2b and 2c is differ-

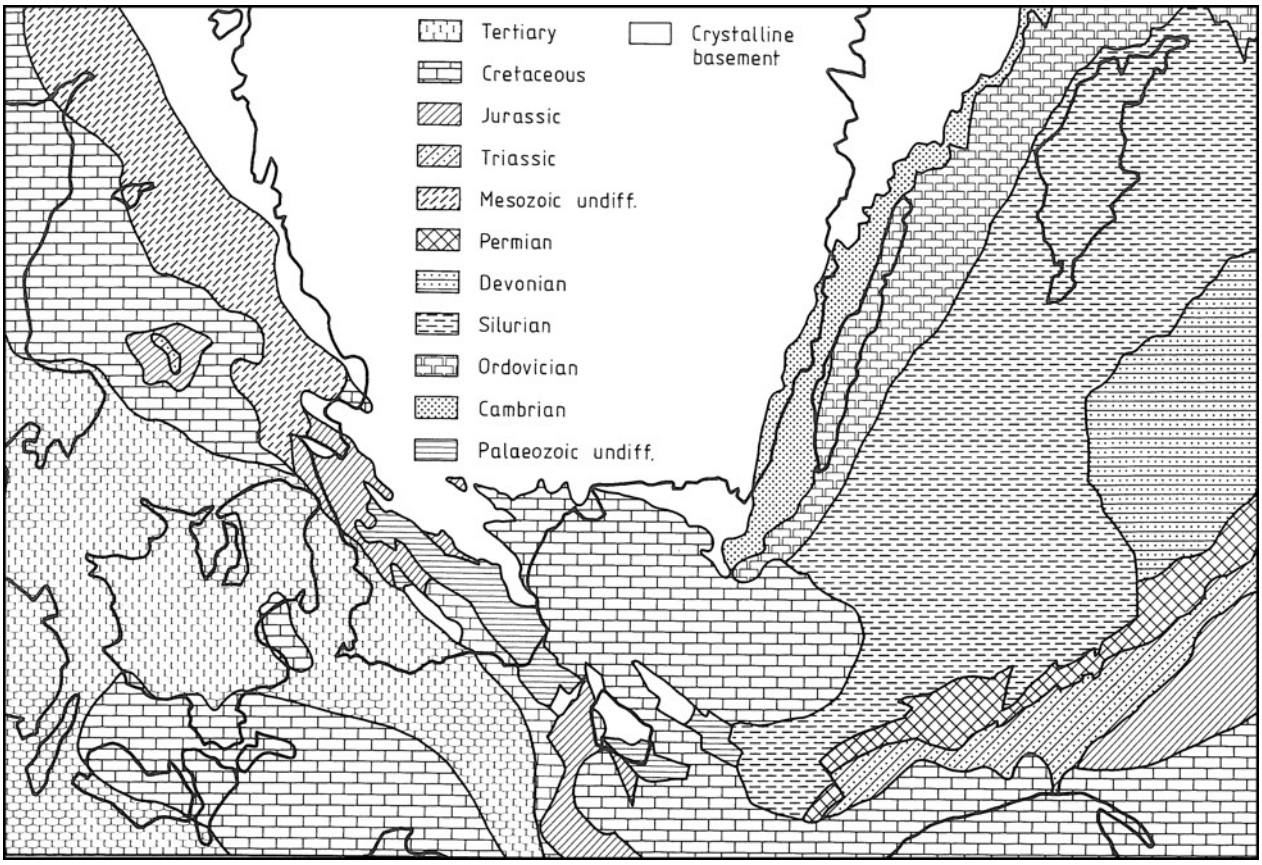

Fig. 20. Map over the pre-Quaternary bedrock in southern Sweden and the Baltic Sea (Ahlberg 1986).

ent from that of unit 1, a deposition in a disintegrating dead-ice environment is the most likely scenario for this depositional stage.

7.3 Stage III: An advancing glacier

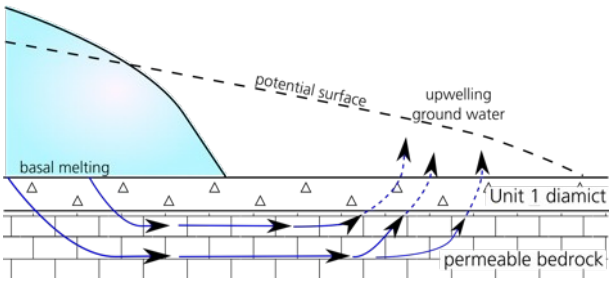

Fig. 21. Generalized sketch on the influence of a diamict with low hydraulic conductivity above a highly conductive limestone aquifer. Modified after Boulton & Caban (1995).

The next stage is related to changes in the strength of existing sediments and their deformation. The combination and superposition of different deformation structures and styles in chronological order can be explained by the effects of an advancing ice.

The interpretation is based mainly on the models of subglacial and ice-marginal groundwater flow as proposed by Boulton & Caban (1995) and Rijsdijk et al. (1999). The general groundwater flow at an ice margin is from a high hydraulic potential below a glacier towards a low potential at the ice front (Fig. 21).

Directly beneath the ice margin, upwelling of groundwater was prevented by the low permeability of the till in unit 1. This blocking lead to the buildup of a high pore water pressure beneath the unit 1 till in front of the glacier. This increase in subglacial water pressure lowered the shear strength of the till which in some places became liquified. The pushing by the advancing ice against the weakened till lead to initial buckling of the glacier foreland (Croot 1988).

When the pressure difference between the water below the diamict and the atmosphere was large enough, upward seepage of the ground water started. This upward groundwater flow lead to the fluidization of the lower till, to diapirism due to decreased density (Leeder 1982, p. 114) and to hydrofracturing (Boulton & Caban 1995, Rijsdijk et al. 1999).

Two different possibilities exist to explain the exceptional composition of Subunit 2d which contains clasts of porous limestone in a matrix of fine sand and silt. Either

the material was transported in suspension as a flow on the surface from an unknown source or it was washed out by upwelling water from the till in unit 1. In both cases, the flow (probably with a slurry-like appearance) must be highly saturated with sediment, otherwise the granule sized limestone clasts could not be transported in suspension. Outwash from unit 1 can happen if a strong upward water flow is created through unit 1 which takes the fine fractions and the low-density larger clasts (Fig. 19, step III, 3).

The primary sediment structures in Subunit 2e indicate an unidirectional flow. This flow was probably a surface flow of the upwelling water which flooded the glacier foreland (Fig. 19, stage III, 4). The calcite-beds were deposited when the pressurized water reached the surface and the pressure dropped.

The diamict in Subunit 3a could either be deposited as debris flows in front of the advancing glacier or below the glacier snout during an ice advance. The preserved primary structures in Subunit 2e and the calcite-beds exclude a glacier deforming its bed.

7.4 Stage IV: a second Baltic ice stream

The uppermost part of the section is interpreted to represent the subglacial environment below a Baltic ice stream.

The advancing glacier was deforming and eroding preexisting sediments and the ice must then have been coupled to its bed. The lower part of unit 3 shows in general a low degree of homogenization, as can be seen from the preserved intraclasts that form boudinage structures in Subunit 3b. This is evidence for simple shear deformation (McCarroll & Rijsdijk 2003) which occurs beneath active ice. For further discussion on bed deformation, see stage I.

Unit 3 contains less local limestone than unit 1, while the relative amount of far-travelled limestone is almost the same in both units. In general, no new lithologies appear in unit 3, and the lithologic composition is interpreted to be the result of mixing of both lower units (1 and 2).

Clast fabric indicates an ice advance from the south. Further support for this stress direction are the overturned folds in unit 2e at *c.* 8 m (Fig. 11) which indicate deformation by shear stress induced by a glacier advancing from the south.

As unit 3 continues to the present terrain surface, it can be stated that the deglaciation phase did not leave any sediment (seen in the section). There are no signs for the ice of this last ice stream being debris laden and forming a dead-ice landscape.

8 Regional implications

The geomorphological map (Fig. 5) shows two distinctly different landscape types, one with a flat, slightly undulating surface and one with hummocky landforms. The area around Vellinge is situated in the flat area and the sediments observed in Vellinge fit to the general description of the stratigraphy in the southwestern coastal plain as presented by Ringberg (1975). He described two tills of Baltic provenance on top of the bedrock between Malmö and Vellinge, a thin upper till (0.5–2.2 m; Ringberg 1975, p. 27) and a lower till of varying (but generally less than 15 m) thickness (Ringberg 1975, p. 29). In some places he found the two tills to be separated by sandy to silty sediments and in some places a third till has been found. Ringberg (1988) also described two Baltic tills for Söderslätt, the plain along the southern coast. The two till units were not identified everywhere in the geological profiles (Fig. 4) but discontinuous layers of sand sometimes occur between an upper and a lower till.

A succession of two ice advances separated by a period of ice stagnation and dead-ice melting is suggested for the entire coastal area in south-western Scania. These periods represent the latest part of the late Weichselian history in the area. The deformation tills indicate rapidly flowing ice-streams, the first with an ice-flow direction as observed in Vellinge from south-east and the second from the south.

The hummocky terrain further inland differs significantly from the coastal plains (Fig. 5). The stratigraphy of those hummocks is more complex and the debris has a different provenance (Nilsson 1959). According to the depositional model proposed by Nilsson (1959), the hummocky area was overridden by ice from the first advance of the late Weichselian, which came from NNE and then turned to NE. The first dead-ice area was decoupled on the lee-side (SW) of the Romeleåsen horst (Fig. 2), at the same time as ice flow in active ice changed to a more easterly direction and became the young-Baltic ice stream which continued on the southern side of the decoupled dead-ice area. A gradual change from an easterly to a more southerly ice-flow direction lead to a gradual detachment of more dead-ice and accretion of more such along the southern part of the initial dead-ice area (Nilsson 1959). After the southernmost low-baltic part of the dead ice was separated from the active ice, the ice-stream continued its flow along the western coast of Scania. According to this model, active ice was diverted by dead-ice in a clockwise direction, from N, NE, E, SE, and finally from the south.

According to its morphology, the hummocky terrain can be divided in two different areas (Nilsson 1959; Ringberg 1980; Lidmar-Bergström et al. 1991), a northern part with large hummocks (height differences 25–50 m, Ringberg 1980) and a southern part with smaller hummocks (height differences < 10 m).

Nilsson (1959) suggested that the low-Baltic ice only reached the latter area and did not affect the former. From existing data is it not possible to distinguish exactly which ice advance left the dead-ice in the area with the smaller hummocks, but it is very likely that the area was covered by dead-ice, diverting the ice advance depositing unit 3 in Vellinge. This dead-ice diverted the ice stream (by the same processes as described by Nilsson (1959) for the earlier stages) to the coastal plains and was not overridden by the glacier. If it would have been overridden, the landforms would have been changed and probably look more like the ones in the coastal plains. The fact that it was diverted by dead-ice is a sign for a thin ice stream as a thick one would not be that dependent on the topography.

We have also clear indication that the area around Vellinge was ice free between the two ice advances, so that the sediments in unit 2 could be deposited. This can be explained by a thin dead-ice left behind by the penultimate advance. A thin ice cover had time to melt before the new advance reached the area, making space for the proglacial environment as discussed in chapter 7.3. The dead-ice left along the southern coast, in the parts that form the smaller hummocks today, was probably thicker and did not have time to melt before the most recent advance.

This reconstruction strongly contradicts Houmark-Nielsen & Kjær's (2003) interpretation. They suggested that almost all of Scania was affected by the last active ice advance from the south (Fig. 1 B). If that would have been the case, none of the hummocks would be preserved but rather be reshaped subglacially. Their model also requires a steep gradient and relatively thick ice, while the one proposed by Ringberg (1989, Fig. 1 A) implies a thin ice with a low gradient and a rapid deglaciation once the ice became inactive.

A thin, highly dynamic ice is supported by the findings of the present study. Such high ice dynamics have also been reported from other sites close to the study area, for example by Adrielsson (2001) who proposed surging ice lobes protruding from a generally retreating ice sheet. This fits also with the interpretation by Ringberg (1988), stating that the Low Baltic ice was the last influential ice from the Baltic depression and that there were no new Baltic ice streams thereafter.

The two active phases interpreted from the section in Vellinge represent the two latest young-Baltic ice-lobe advances over eastern Denmark and Scania, probably the Bælthav advance and the Öresund Advance (Kjær et al. 2003).

9 Conclusions

- The study area contains both plains along the southern and western coasts and a hummocky landscape further inland. The hummocky area represents deposition from dead-ice while the coastal plains have been formed in the subglacial environment beneath rapidly advancing ice.
- Sediments representing two different ice advances separated by ice stagnation and dead-ice melting have been investigated in Vellinge. The last ice advance eroded previously deposited sediments.
- The ice advances were thin ice streams from the Baltic basin. They were diverted to the coastal areas by dead-ice left behind by earlier advances and did not override the hummocky landscape.

10 Acknowledgements

Thanks are mainly due to my supervisors, Lena Adrielsson and Nicolaj Krog Larsen and to Johanna Anjar who provided interesting discussions and explanations both in the field and during later stages of the project. People at the branch office of SGU in Lund provided data from the well archive and information on their suitability for the intended purposes.

References

Adrielsson, L. (2001): Subglacial hydrology and bed deformation dynamics during a Late Weichselian ice lobe surge in the Öresund strait area, south Scandinavia. *In Palaeo–Ice Stream International Symposium 17–20 Oct. 2001*.

Adrielsson, L., Barnekow, L., Björkman, L., Holmström, P. & Lagerås, P. (1989): Glacial sedimentologi och miljöanalys av kvartära lager i Limhamns kalkbrott, Skåne. Projektrapport Kvartärgeologi KV 611, Lunds Universitet.

Ahlberg, P. (1986): *Den Svenska kontinentalsockelns berggrund*. SGU Rapporter & Meddelanden 47, Uppsala.

Benn, D. I. (1994): Fabric shape and the interpretation of sedimentary fabric data. *Journal of Sedimentary Research A64*, 910–915.

Benn, D. I. (1995): Fabric signature of subglacial till deformation, Breidamerkurjökull, iceland. *Sedimentology 42*, 735–747.

Benn, D. I. & Evans, D. J. A. (2010): *Glaciers & Glaciation*. Hodder Education, London, 2nd edn..

Boulton, G. S. & Caban, P. (1995): Groundwater flow beneath ice sheets: Part II — Its impact on glacier tectonic structures and moraine formation. *Quaternary Science Reviews 14*, 563–587.

Boulton, G. S., Dobbie, K. E. & Zatsepin, S. (2001): Sediment deformation beneath glaciers and its coupling to the subglacial hydraulic system. *Quaternary International 86*, 3–28.

Boulton, G. S. & Hindmarsh, R. C. A. (1987): Sediment deformation beneath glaciers: rheology and sedimentological consequences. *Journal of Geophysical Research 92*(B9), 9059–9082.

Bridgland, D. (ed.) (1986): *Clast lithographical analysis*. Quaternary Research Association Technical Guide 3, Cambridge.

Croot, D. G. (1988): Morphological, structural and mechanical analysis of neoglacial ice-pushed ridges in Iceland. *In* D. G. Croot (ed.) *Glaciotectonics: Forms and Processes*, 33–47, A. A. Balkema.

Daniel, E. (1977): *Beskrivning till kartbladet Trelleborg NO*. SGU Ae33, Stockholm.

Deutsches Institut für Normung (2003): Geotechnische Erkundung und Untersuchung–Benennung, Beschreibung und Klassifizierung von Fels–Teil 1: Benennung und Beschreibung (ISO 14689-1:2003). Tech. Rep., DIN.

Dowdeswell, J. A. & Sharp, M. J. (1986): Characterization of pebble fabrics in modern terrestrial glacigenic sediments. *Sedimentology 33*, 699–710.

Ehlers, J. (1979): Fine gravel analysis after the Dutch method as tested out on Ristinge Klint, Denmark. *Bulletin of the Geological Society of Denmark 27*, 157–164.

Evans, D. J. A. & Benn, D. I. (eds.) (2004): *A practical guide to the study of glacial sediments*. Arnold, London.

Evans, D. J. A., Phillips, E. R., Hiemstra, J. F. & Auton, C. A. (2006): Subglacial till: Formation, sedimentary characteristics and classification. *Earth–Science Reviews 78*, 115–176.

Hallet, B. (1976): Deposites formed by subglacial precipitation of $CaCO_3$. *Geological Society of America Bulletin 87*, 1003–1015.

Holmström, L. (1896): Studier öfver de lösa jordlagren vid egendomen Klågerup i Skåne. *Geologiska Föreningens i Stockholm. Förhandlingar 18*.

Holmström, L. (1899): Geologisk profil från Åkarp till Lomma. *Geologiska Föreningens i Stockholm. Förhandlingar 21*.

Holmström, L. (1904): Öfversikt af den glaciala afslipningen i Sydskandinavien. *Geologiska Föreningens i Stockholm. Förhandlingar 26*.

Holst, N. O. (1895): *Beskrifning till kartbladet Skanör*. SGU Aa112, Stockholm.

Holst, N. O. (1903): *Om skrifkritan i Tulltorpstrakten och de båda moräner, i hvilka den är inbäddad*. SGU C194, Stockholm.

Holst, N. O. (1911a): *Alnarpsfloden*. SGU C237, Stockholm.

Holst, N. O. (1911b): *Beskrifning till kartbladet Börringekloster*. SGU Aa138, Stockholm.

Hooyer, T. S. & Iverson, N. R. (2000): Clast-fabric development in a shearing granular material: Implications for subglacial till and fault gouge. *Geological Society of America Bulletin 112*, 683–692.

Houmark-Nielsen, M. (1999): A lithostratigraphy of Weichselian glacial and interstadial deposits in Denmark. *Bulletin of the Geological Society of Denmark 46*, 101–114.

Houmark-Nielsen, M. & Kjær, K. H. (2003): Southwest Scandinavia, 40–15 kyr BP:palaeogeography and environmental change. *Journal of Quaternary Science 18*(8), 769–786.

Jarvis, A., Reuter, H. I., Nelson, A. & Guevara, E. (2008): *Hole-filled SRTM for the globe Version 4*. available from the CGIAR-CSI SRTM 90m Database: http://srtm.csi.cgiar.org.

Jönsson, K. M. (2000): *Sedimentologiska och litostratigrafiska undersökningar i södra Malmös kvartära avlagringar, södra Sverige*. Examensarbete i Geologi vid Lunds Universitet, Nr. 117.

Kjær, K. H., Houmark-Nielsen, M. & Richardt, N. (2003): Ice-flow patterns and dispersal of erratics at the southwestern margin of the last Scandinavian Ice Sheet: signature of palaeo-ice streams. *Boreas 32*, 130–148.

Kjær, K. H., Lagerlund, E., Adrielsson, L., Puthussery, J. T., Murray, A. S. & Sandgren, P. (2006): The first independent chronology for Middle and Late Weichselian sediments from southern Sweden and the island of Bornholm. *GFF 128*, 209–220.

Lagerlund, E. (1977a): *Förutsättningar för moränstratigrafiska undersökningar på Kullen i Nordvästskåne*. Univ. Lund, Dept. of Quat. Geol. LUNDQUA Thesis 5.

Lagerlund, E. (1977b): Till studies and neotectonics in northwest Skåne, south Sweden. *Boreas 6*, 159–166.

Lagerlund, E. (1987): An alternative Weichselian glaciation model with special reference to the glacial history of Skåne, South Sweden. *Boreas 16*, 433–459.

Larsen, N. K., Knudsen, K. L., Krohn, C. F., Kronborg, C., Murray, A. S. & Nielsen, O. B. (2009): Late Quaternary ice sheet, lake and sea history of southwest Scandinavia – a synthesis. *Boreas 38*(4), 732–761.

Le Heron, D. P. & Etienne, J. L. (2005): A complex subglacial clastic dyke swarm, Sólheimajökull, southern Iceland. *Sedimentary Geology 181*, 25–37.

Leeder, M. R. (1982): *Sedimentology: process and product*. Allen & Unwin, London.

Lidmar-Bergström, K., Elvhage, C. & Ringberg, B. (1991): Landforms in Skåne, south Sweden. Preglacial and glacial landforms analysed from two relief maps. *Geografiska Annaler 73A*(2), 61–91.

Malmberg Persson, K. & Lagerlund, E. (1990): Sedimentology and depositional environments of the Lund Diamicton, southern Sweden. *Boreas 19*(2), 181–199.

McCarroll, D. & Rijsdijk, K. F. (2003): Deformation styles as a key for interpreting glacial depositional environments. *Journal of Quaternary Science 18*(6), 473–489.

Mulder, T. & Alexander, J. (2001): The physical character of subaqueous sedimentary density flows and their deposits. *Sedimentology 48*, 269–299.

Munthe, H., Johansson, H. E. & Grönwall, K. A. (1920): *Beskrivning till kartbladet Sövdeborg*. SGU Aa142, Stockholm.

Nilsson, K. (1959): *Isströmmar och isavsmältning i sydvästra Skånes backlandskap*. SGU C567, Stockholm.

Paterson, W. S. B. (1994): *The physics of glaciers*. Butterworth-Heinemann, Oxford, Birlington, 3rd edn..

Rijsdijk, K. F., Owen, G., Warren, W. P., McCarroll, D. & van der Meer, J. J. (1999): Clastic dykes in overconsolidated tills: evidence for subglacial hydrofracturing at Killiney Bay, eastern Ireland. *Sedimentary Geology 129*, 111–126.

Ringberg, B. (1975): *Beskrivning till kartbladet Trelleborg NV/Malmö SV*. SGU Ae23, Stockholm.

Ringberg, B. (1980): *Beskrivning till kartbladet Malmö SO*. SGU Ae38, Uppsala.

Ringberg, B. (1988): Late Weichselian geology of southernmost Sweden. *Boreas 17*, 243–263.

Ringberg, B. (1989): Upper Late Weichselian lithostratigraphy in western Skåne, southernmost Sweden. *Geologiska Föreningens i Stockholm. Förhandlingar 111*(4), 319–337.

Ringberg, B. (2003): Readvance and retreat of the Late Weichselian Low Baltic ice stream in southernmost Sweden – a review. *GFF 125*, 169–176.

Selley, R. C. (1976): *An introduction to sedimentology*. Academic Press, London.

Slaymaker, O. (2009): Proglacial, periglacial or paraglacial. *In* J. Knight & S. Harrison (eds.) *Periglacial and Paraglacial Processes and Environments*, vol. 320, 71–84, Geological Society, London.

Truffer, M. & Echelmeyer, K. A. (2003): Of isbræ and ice streams. *Annals of Glaciology 36*, 66–72.

Waller, R. I. (2001): The influence of basal processes on the dynamic behaviour of cold–based glaciers. *Quaternary International 86*, 117–128.

Van der Wateren, F. M., Kluiving, S. J. & Bartek, L. R. (2000): Kinematic indicators of subglacial shearing. *In* A. J. Maltman, B. Hubbard & M. J. Hambrey (eds.) *Deformation of Glacial Materials*, 259–278, Geological Society, London.

Willis, I. C. (1995): Intra-annual variations in glacier motion: a review. *Progress in Physical Geography 19*, 61–106.

Appendix

A Section drawing

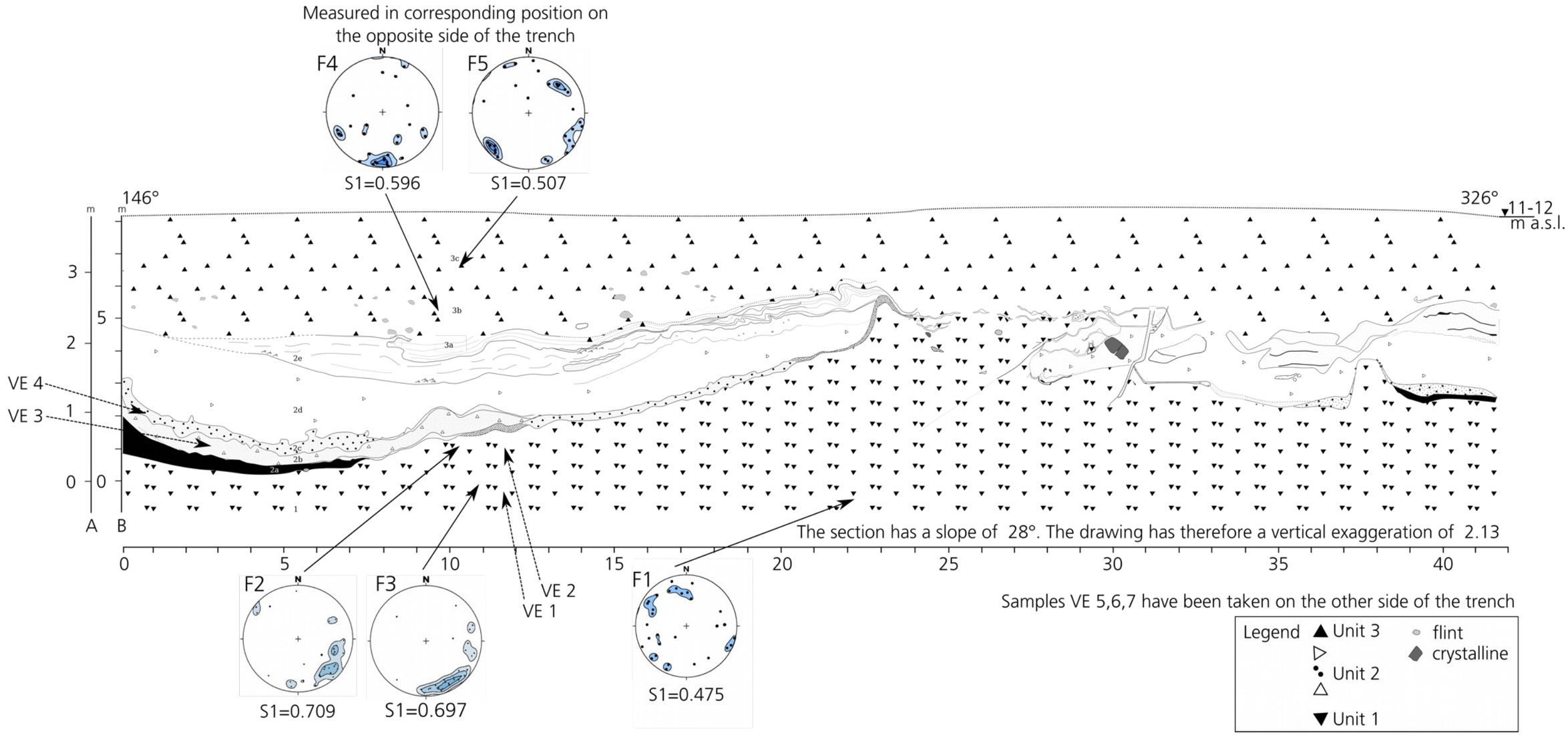

B Grain size

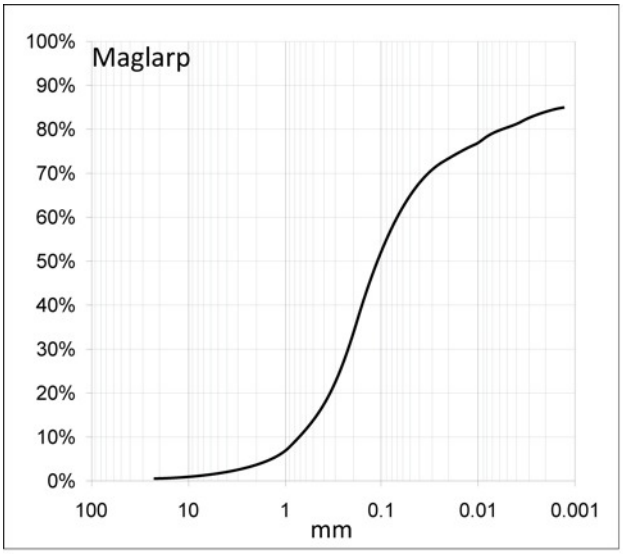

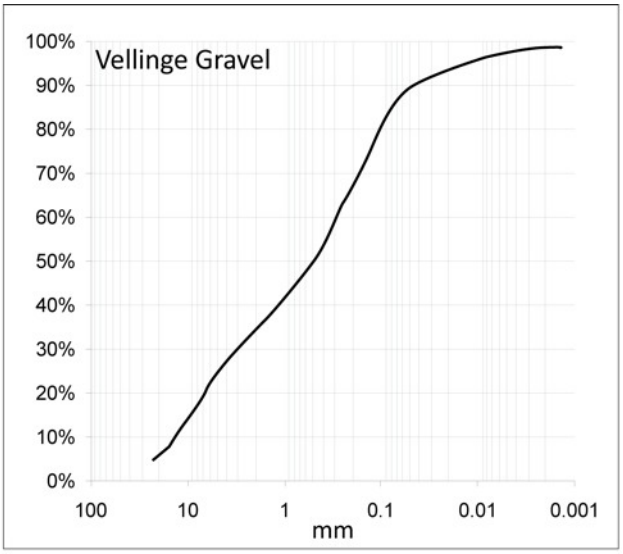

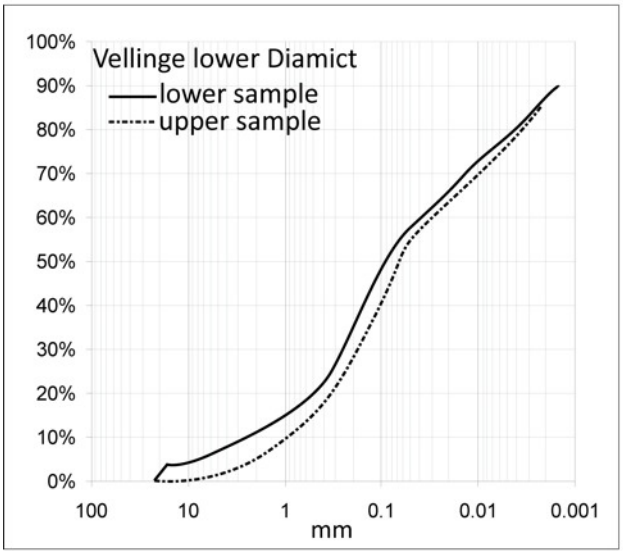

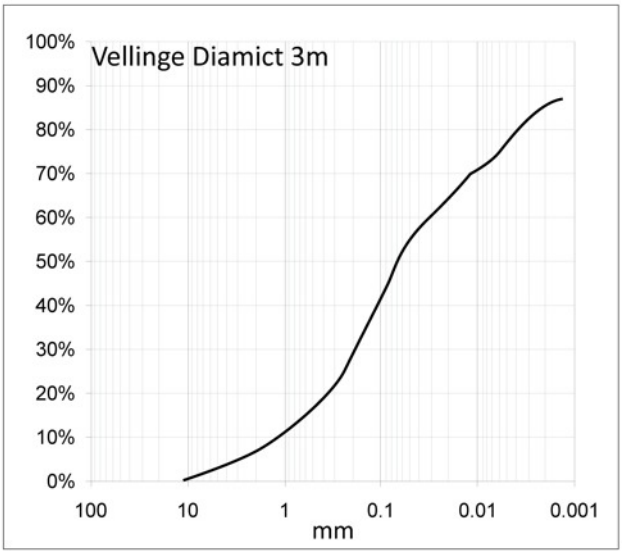

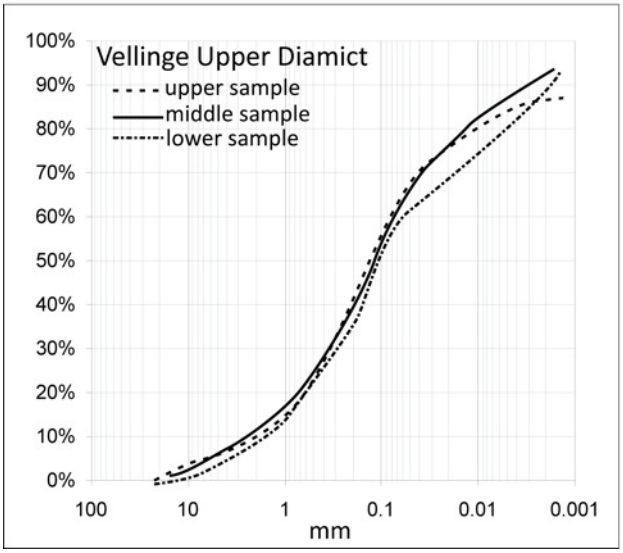

Grain sizes 22.4 to 0.063 mm were measured by sieving, finer grain sizes were measured with hydrometers in sedimentation columns.

Sample	Clay	Silt	Sand	Gravel
VE1	15	30	43	12
VE2	15	32	47	6
VE3	14	34	44	8
VE4	1	11	54	34
VE5	12	28	48	12
VE6	8	26	55	11
VE7	13	22	55	10

Tab. 1. Numerical values (%) for the grain size distribution as used for Fig. 9 and 10.

C Fine gravel data

Sample	Qz	Cry	Fl	SSt	FSSt	SiSt	Pal LS	CT LS	Oth	Sum	Sum NLS	Sum LS
Änghög upper	20	104	22	47	0	61	80	39	2	373	254	119
Änghög lower	24	151	26	36	10	27	140	52	1	466	274	192
Anderslöv upper	15	231	16	33	23	43	1	0	3	362	361	1
Anderslöv lower	22	283	19	49	16	55	33	19	0	496	444	52
Håslöv 1	12	126	38	58	22	36	12	5	11	309	292	17
Håslöv 2	18	195	43	49	17	35	110	117	0	584	357	227
Skegrie 1	43	217	39	33	6	72	0	0	10	410	410	0
Skegrie 2	54	293	52	58	10	217	0	0	30	684	684	0
Maglarp	26	230	49	43	2	103	0	0	30	483	453	0
VE7	45	367	67	92	22	56	38	28	41	756	649	66
VE6	20	179	38	63	17	49	100	80	11	557	366	180
VE5	18	110	26	50	9	34	90	74	0	411	247	164
VE4	26	153	6	49	10	81	140	20	8	493	325	160
VE3	55	196	0	39	6	56	156	2 6	516	352	158	
VE2	15	141	22	22	6	16	117	150	0	489	222	267
VE1	18	147	23	25	2	47	104	163	4	533	262	267
VE8	25	180	39	73	24	17	131	113	0	602	358	244

Tab. 2. This table shows the raw numbers for the different lithologies for the samples that were analysed in this study. It shows also total sum, and the sums for non-calcareous and calcareous lithologies, respectively. Lithology abbreviations: Qz: Quartz; Cry: Crystalline rocks; Fl: Flint; SSt: Sandstone; FSSt: Fine sandstone; SiSt: Siltstone; Pal LS: Palaeozoic limestone; CT LS: cretaceous-/ tertiary limestone; Oth: unidentified lithologies

Sample	Qz	Cry	Fl	SSt	FSSt	SiSt	Pal LS	CT LS	Others
Änghög upper	5,36%	27,88%	5,90%	12,60%	0,00%	16,35%	21,45%	10,46%	0,54%
Änghög lower	5,15%	32,40%	5,58%	7,73%	2,15%	5,79%	30,04%	11,16%	0,21%
Anderslöv upper	4,14%	63,81%	4,42%	9,12%	6,35%	11,88%	0,28%	0,00%	0,83%
Anderslöv lower	4,44%	57,06%	3,83%	9,88%	3,23%	11,09%	6,65%	3,83%	0,00%
Håslöv 1	3,88%	40,78%	12,30%	18,77%	7,12%	11,65%	3,88%	1,62%	3,56%
Håslöv 2	3,08%	33,39%	7,36%	8,39%	2,91%	5,99%	18,84%	20,03%	0,00%
Skegrie 1	10,49%	52,93%	9,51%	8,05%	1,46%	17,56%	0,00%	0,00%	2,44%
Skegrie 2	7,89%	42,84%	7,60%	8,48%	1,46%	31,73%	0,00%	0,00%	4,39%
Maglarp	5,38%	47,62%	10,14%	8,90%	0,41%	21,33%	0,00%	0,00%	6,21%
VE7	5,95%	48,54%	8,86%	12,17%	2,91%	7,41%	5,03%	3,70%	5,42%
VE6	3,59%	32,14%	6,82%	11,31%	3,05%	8,80%	17,95%	14,36%	1,97%
VE5	4,38%	26,76%	6,33%	12,17%	2,19%	8,27%	21,90%	18,00%	0,00%
VE4	5,27%	31,03%	1,22%	9,94%	2,03%	16,43%	28,40%	4,06%	1,62%
VE3	10,66%	37,98%	0,00%	7,56%	1,16%	10,85%	30,23%	0,39%	1,16%
VE2	3,07%	28,83%	4,50%	4,50%	1,23%	3,27%	23,93%	30,67%	0,00%
VE1	3,38%	27,58%	4,32%	4,69%	0,38%	8,82%	19,51%	30,58%	0,75%
VE8	4,15%	29,90%	6,48%	12,13%	3,99%	2,82%	21,76%	18,77%	0,00%

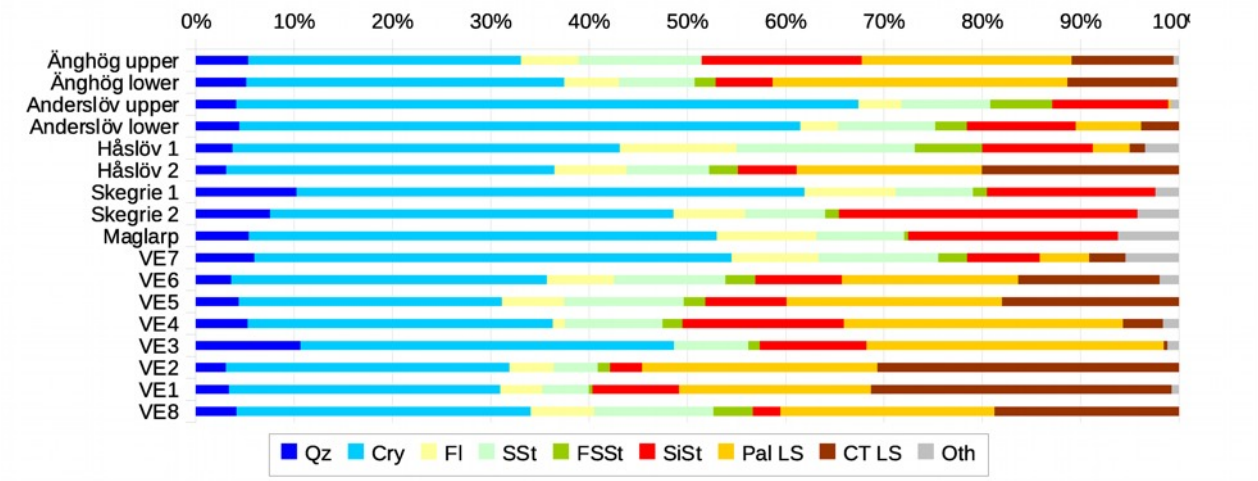

Tab. 3. Percentage values for the different lithologies in the fine gravel fraction calculated following the 'Swedish' method, i.e. without putting the stable and the non-stable lithologies into separate groups. Lithology abbreviations: Qz: Quartz; Cry: Crystalline rocks; Fl: Flint; SSt: Sandstone; FSSt: Fine sandstone; SiSt: Siltstone; Pal LS: Palaeozoic limestone; CT LS: cretaceous-/ tertiary limestone; Others: unidentified lithologies

Sample	Qz	Cry	Fl	SSt	FSSt	SiSt	Pal LS	CT LS	Others
Änghög upper	7,87%	40,94%	8,66%	18,50%	0,00%	24,02%	31,50%	15,35%	0,79%
Änghög lower	8,76%	55,11%	9,49%	13,14%	3,65%	9,85%	51,09%	18,98%	0,36%
Anderslöv upper	4,16%	63,99%	4,43%	9,14%	6,37%	11,91%	0,28%	0,00%	0,83%
Anderslöv lower	4,95%	63,74%	4,28%	11,04%	3,60%	12,39%	7,43%	4,28%	0,00%
Håslöv 1	4,11%	43,15%	13,01%	19,86%	7,53%	12,33%	4,11%	1,71%	3,77%
Håslöv 2	5,04%	54,62%	12,04%	13,73%	4,76%	9,80%	30,81%	32,77%	0,00%
Skegrie 1	10,49%	52,93%	9,51%	8,05%	1,46%	17,56%	0,00%	0,00%	2,44%
Skegrie 2	7,89%	42,84%	7,60%	8,48%	1,46%	31,73%	0,00%	0,00%	4,39%
Maglarp	5,74%	50,77%	10,82%	9,49%	0,44%	22,74%	0,00%	0,00%	6,62%
VE7	6,93%	56,55%	10,32%	14,18%	3,39%	8,63%	5,86%	4,31%	6,32%
VE6	5,46%	48,91%	10,38%	17,21%	4,64%	13,39%	27,32%	21,86%	3,01%
VE5	7,29%	44,53%	10,53%	20,24%	3,64%	13,77%	36,44%	29,96%	0,00%
VE4	8,00%	47,08%	1,85%	15,08%	3,08%	24,92%	43,08%	6,15%	2,46%
VE3	15,63%	55,68%	0,00%	11,08%	1,70%	15,91%	44,32%	0,57%	1,70%
VE2	6,76%	63,51%	9,91%	9,91%	2,70%	7,21%	52,70%	67,57%	0,00%
VE1	6,87%	56,11%	8,78%	9,54%	0,76%	17,94%	39,69%	62,21%	1,53%
VE8	6,98%	50,28%	10,89%	20,39%	6,70%	4,75%	36,59%	31,56%	0,00%

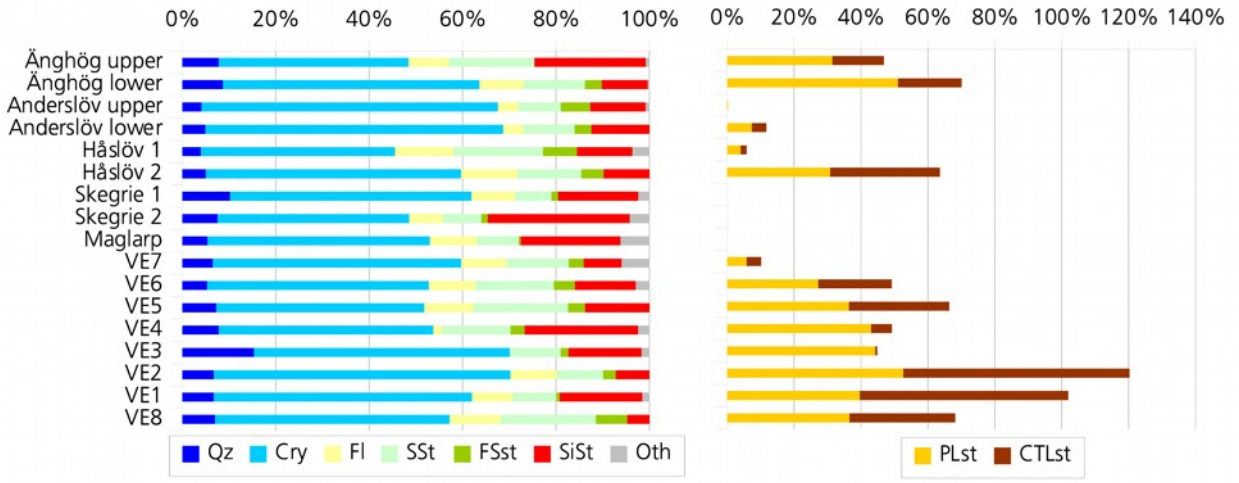

Tab. 4. Percentage values for the different lithologies in the fine gravel fraction calculated following the Danish method; i.e. normalizing the stable lithologies to 100% and calculating the non-stable lithologies relatively to the stable lithologies. Lithology abbreviations: Qz: Quartz; Cry: Crystalline rocks; Fl: Flint; SSt: Sandstone; FSSt: Fine sandstone; SiSt: Siltstone; Pal LS: Palaeozoic limestone; CT LS: cretaceous-/ tertiary limestone; Others: unidentified lithologies

Sample	Qz	Cry	Fl	SSt	FSSt	SiSt	Pal LS	CT LS	Others
Änghög upper	7,87%	40,94%	8,66%	18,50%	0,00%	24,02%	21,45%	10,46%	0,54%
Änghög lower	8,76%	55,11%	9,49%	13,14%	3,65%	9,85%	30,04%	11,16%	0,21%
Anderslöv upper	4,16%	63,99%	4,43%	9,14%	6,37%	11,91%	0,28%	0,00%	0,83%
Anderslöv lower	4,95%	63,74%	4,28%	11,04%	3,60%	12,39%	6,65%	3,83%	0,00%
Håslöv 1	4,11%	43,15%	13,01%	19,86%	7,53%	12,33%	3,88%	1,62%	3,56%
Håslöv 2	5,04%	54,62%	12,04%	13,73%	4,76%	9,80%	18,84%	20,03%	0,00%
Skegrie 1	10,49%	52,93%	9,51%	8,05%	1,46%	17,56%	0,00%	0,00%	2,44%
Skegrie 2	7,89%	42,84%	7,60%	8,48%	1,46%	31,73%	0,00%	0,00%	4,39%
Maglarp	5,74%	50,77%	10,82%	9,49%	0,44%	22,74%	0,00%	0,00%	6,21%
VE7	6,93%	56,55%	10,32%	14,18%	3,39%	8,63%	5,03%	3,70%	5,42%
VE6	5,46%	48,91%	10,38%	17,21%	4,64%	13,39%	17,95%	14,36%	1,97%
VE5	7,29%	44,53%	10,53%	20,24%	3,64%	13,77%	21,90%	18,00%	0,00%
VE4	8,00%	47,08%	1,85%	15,08%	3,08%	24,92%	28,40%	4,06%	1,62%
VE3	15,63%	55,68%	0,00%	11,08%	1,70%	15,91%	30,23%	0,39%	1,16%
VE2	6,76%	63,51%	9,91%	9,91%	2,70%	7,21%	23,93%	30,67%	0,00%
VE1	6,87%	56,11%	8,78%	9,54%	0,76%	17,94%	19,51%	30,58%	0,75%
VE8	6,98%	50,28%	10,89%	20,39%	6,70%	4,75%	21,76%	18,77%	0,00%

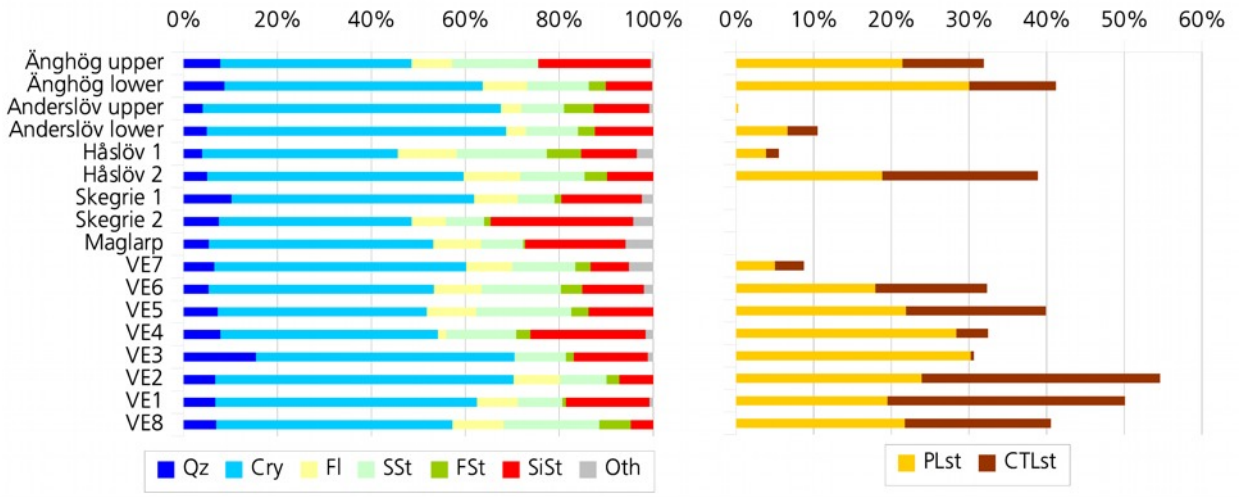

Tab. 5. Percentage values for the different lithologies in the fine gravel fraction calculated following the Danish method; i.e. normalizing the stable lithologies to 100% and (in contrast to Tab.3), calculating the amount of non-stable lithologies relative to the total number of grains in the sample. Lithology abbreviations: Qz: Quartz; Cry: Crystalline rocks; Fl: Flint; SSt: Sandstone; FSSt: Fine sandstone; SiSt: Siltstone; Pal LS: Palaeozoic limestone; CT LS: cretaceous-/ tertiary limestone; Others: unidentified lithologies

Tidigare skrifter i serien ”Examensarbeten i Geologi vid Lunds Universitet”:

223. Stefanowicz, Sissa, 2008: Palynostratigraphy and palaeoclimatic analysis of the Lower - Middle Jurassic (Pliensbachian - Bathonian) of the Inner Hebrides, NW Scotland. (15 hskp)
224. Holm, Sanna, 2008: Variations in impactor flux to the Moon and Earth after 3.85 Ga. (15 hskp)
225. Bjärnborg, Karolina, 2008: Internal structures in detrital zircons from Hamrånge: a study of cathodoluminescence and back-scattered electron images. (15 hskp)
226. Noresten, Barbro, 2008: A reconstruction of subglacial processes based on a classification of erosional forms at Ramsvikslandet, SW Sweden. (30 hskp)
227. Mehlqvist, Kristina, 2008: En mellanjurassisk flora från Bagå-formationen, Bornholm. (15 hskp)
228. Lindvall, Hanna, 2008: Kortvariga effekter av tefranedfall i lakustrin och terrestrisk miljö. (15 hskp)
229. Löfroth, Elin, 2008: Are solar activity and cosmic rays important factors behind climate change? (15 hskp)
230. Damberg, Lisa, 2008: Pyrit som källa för spårämnen – kalkstenar från övre och mellersta Danien, Skåne. (15 hskp)
331. Cegrell, Miriam & Mårtensson, Jimmy, 2008: Resistivity and IP measurements at the Bolmen Tunnel and Ådalsbanan, Sweden. (30 hskp)
232. Vang, Ina, 2008: Skarn minerals and geological structures at Kalkheia, Kristiansand, southern Norway. (15 hskp)
233. Arvidsson, Kristina, 2008: Vegetationen i Skandinavien under Eem och Weichsel samt fallstudie i submoräna organiska avlagringar från Nybygget, Småland. (15 hskp)
234. Persson, Jonas, 2008: An environmental magnetic study of a marine sediment core from Disko Bugt, West Greenland: implications for ocean current variability. (30 hskp)
235. Holm, Sanna, 2008: Titanium- and chromium-rich opaque minerals in condensed sediments: chondritic, lunar and terrestrial origins. (30 hskp)
236. Bohlin, Erik & Landen, Ludvig, 2008: Geofysiska mätmetoder för prospektering till ballastmaterial. (30 hskp)
237. Brodén, Olof, 2008: Primär och sekundär migration av hydrokarboner. (15 hskp)
238. Bergman, Bo, 2009: Geofysiska analyser (stångslingram, CVES och IP) av lagerföljd och lakvattenrörelser vid Albäcksdeponin, Trelleborg. (30 hskp)
239. Mehlqvist, Kristina, 2009: The spore record of early land plants from upper Silurian strata in Klinta 1 well, Skåne, Sweden. (45 hskp)
239. Mehlqvist, Kristina, 2009: The spore record of early land plants from upper Silurian strata in Klinta 1 well, Skåne, Sweden. (45 hskp)
240. Bjärnborg, Karolina, 2009: The copper sulphide mineralization of the Zinkgruvan deposit, Bergslagen, Sweden. (45 hskp)
241. Stenberg, Li, 2009: Historiska kartor som hjälp vid jordartsgeologisk kartering – en pilotstudie från Vångs by i Blekinge. (15 hskp)
242. Nilsson, Mimmi, 2009: Robust U-Pb baddeleyite ages of mafic dykes and intrusions in southern West Greenland: constraints on the coherency of crustal blocks of the North Atlantic Craton. (30 hskp)
243. Hult, Elin, 2009: Oligocene to middle Miocene sediments from ODP leg 159, site 959 offshore Ivory Coast, equatorial West Africa. (15 hskp)
244. Olsson, Håkan, 2009: Climate archives and the Late Ordovician Boda Event. (15 hskp)
245. Wollein Waldetoft, Kristofer, 2009: Svekofennisk granit från olika metamorfa miljöer. (15 hskp)
246. Månsby, Urban, 2009: Late Cretaceous coprolites from the Kristianstad Basin, southern Sweden. (15 hskp)
247. MacGimpsey, I., 2008: Petroleum Geology of the Barents Sea. (15 hskp)
248. Jäckel, O., 2009: Comparison between two sediment X-ray Fluorescence records of the Late Holocene from Disko Bugt, West Greenland; Paleoclimatic and methodological implications. (45 hskp)
249. Andersen, Christine, 2009: The mineral composition of the Burkland Cu-sulphide deposit at Zinkgruvan, Sweden – a

supplementary study. (15 hskp)

250. Riebe, My, 2009: Spinel group minerals in carbonaceous and ordinary chondrites. (15 hskp)
251. Nilsson, Filip, 2009: Föroreningsspridning och geologi vid Filborna i Helsingborg. (30 hskp)
252. Peetz, Romina, 2009: A geochemical characterization of the lower part of the Miocene shield-building lavas on Gran Canaria. (45 hskp)
253. Åkesson, Maria, 2010: Mass movements as contamination carriers in surface water systems – Swedish experiences and risks.
254. Löfroth, Elin, 2010: A Greenland ice core perspective on the dating of the Late Bronze Age Santorini eruption. (45 hskp)
255. Ellingsgaard, Óluva, 2009: Formation Evaluation of Interlava Volcaniclastic Rocks from the Faroe Islands and the Faroe-Shetland Basin. (45 hskp)
256. Arvidsson, Kristina, 2010: Geophysical and hydrogeological survey in a part of the Nhandugue River valley, Gorongosa National Park, Mozambique. (45 hskp)
257. Gren, Johan, 2010: Osteo-histology of Mesozoic marine tetrapods – implications for longevity, growth strategies and growth rates. (15 hskp)
258. Syversen, Fredrikke, 2010: Late Jurassic deposits in the Troll field. (15 hskp)
259. Andersson, Pontus, 2010: Hydrogeological investigation for the PEGASUS project, southern Skåne, Sweden. (30 hskp)
260. Noor, Amir, 2010: Upper Ordovician through lowermost Silurian stratigraphy and facies of the Borenshult-1 core, Östergötland, Sweden. (45 hskp)
261. Lewerentz, Alexander, 2010: On the occurrence of baddeleyite in zircon in silica-saturated rocks. (15 hskp)
262. Eriksson, Magnus, 2010: The Ordovician Orthoceratite Limestone and the Blommiga Bladet hardground complex at Horns Udde, Öland. (15 hskp)
263. Lindskog, Anders, 2010: From red to grey and back again: A detailed study of the lower Kundan (Middle Ordovician) 'Täljsten' interval and its enclosing strata in Västergötland, Sweden. (15 hskp)
264. Rääf, Rebecka, 2010: Changes in beyrichiid ostracode faunas during the Late Silurian Lau Event on Gotland, Sweden. (30 hskp)
265. Petersson, Andreas, 2010: Zircon U-Pb, Hf and O isotope constraints on the growth versus recycling of continental crust in the Grenville orogen, Ohio, USA. (45 hskp)
266. Stenberg, Li, 2010: Geophysical and hydrogeological survey in a part of the Nhandugue River valley, Gorongosa National Park, Mozambique – Area 1 and 2. (45 hskp)
267. Andersen, Christine, 2010: Controls of seafloor depth on hydrothermal vent temperatures - prediction, observation & 2D finite element modeling. (45 hskp)
268. März, Nadine, 2010: When did the Kalahari craton form? Constraints from baddeleyite U-Pb geochronology and geo-chemistry of mafic intrusions in the Kaapvaal and Zimbabwe cratons. (45 hskp)
269. Dyck, Brendan, 2010: Metamorphic rocks in a section across a Svecnorwegian eclogite-bearing deformation zone in Halland: characteristics and regional context. (15 hskp)
270. McGimpsey, Ian, 2010: Petrology and lithogeochemistry of the host rocks to the Nautanen Cu-Au deposit, Gällivare area, northern Sweden. (45 hskp)
271. Ulmius, Jan, 2010: Microspherules from the lowermost Ordovician in Scania, Sweden – affinity and taphonomy. (15 hskp)
272. Andersson, Josefin, Hybertsen, Frida, 2010: Geologi i Helsingborgs kommun – en geoturistkarta med beskrivning. (15 hskp)
273. Barth, Kilian, 2011:Late Weichselian glacial and geomorphological reconstruction of South-Western Scania, Sweden. (45 hskp)

LUNDS UNIVERSITET

Geologiska enheten
Institutionen för geo- och ekosystemvetenskaper
Sölvegatan 12, 223 62 Lund